TITLE

Mediator 1 ablation induces enamel-to-hair lineage conversion through enhancer dynamics

AUTHOR LIST

Roman Thaler[1,2], Keigo Yoshizaki[3], Thai Nguyen[7], Satoshi Fukumoto[4,5], Pamela Den Besten[6], Daniel D. Bikle[7], Yuko Oda[7]*

AFFILIATIONS

[1] Department of Orthopedic Surgery, Mayo Clinic, Rochester, MN, USA
[2] Center for Regenerative Medicine, Mayo Clinic, Rochester, MN, USA
[3] Section of Orthodontics and Dentofacial Orthopedics, Division of Oral Health, Growth and Development, Kyushu University Faculty of Dental Science, Fukuoka, Japan.
[4] Section of Pediatric Dentistry, Division of Oral Health, Growth and Development, Kyushu University Faculty of Dental Science, Fukuoka, Japan
[5] Division of Pediatric Dentistry, Department of Oral Health and Development Sciences, Tohoku University Graduate School of Dentistry, Sendai, Japan
[6] Department of Dentistry, University of California San Francisco, CA, USA
[7]Departments of Medicine and Endocrinology, University of California San Francisco and Veterans Affairs Health Center San Francisco, CA, USA

ORCID number YO: 0000-0001-6124-3530

* Correspondence to: yuko.oda@ucsf.edu (YO)

Short title: *Med1* controls ectodermal lineage

ABSTRACT

Postnatal cell fate has been postulated to be primarily determined by the local tissue microenvironment. Here, we found that Mediator 1 (*Med1*) dependent epigenetic mechanisms dictate tissue-specific lineage commitment and progression of dental epithelia. Deletion of *Med1*, a key component of the Mediator complex linking enhancer activities to gene transcription, provokes a tissue extrinsic lineage shift, causing hair generation in the dental environment. *Med1* deficiency gives rise to unusual hair growth via primitive cellular aggregates on incisors. Mechanistically, we found that Med1 establishes super-enhancers that control enamel lineage transcription factors in dental stem cells and their progenies. However, *Med1* deficiency reshapes the enhancer landscapes and causes a switch from the dental epithelial transcriptional program towards hair and epidermis on incisors *in vivo,* and in dental epithelial stem cells *in vitro*. *Med1* loss also provokes an increase in the number and size of enhancers. Interestingly, control dental epithelia already exhibit enhancers for hair and epidermal key transcription factors; these expand in size and transform into active super-enhancers upon *Med1* loss suggesting that these epigenetic mechanisms cause the transcriptomic and phenotypic shift towards epidermal and hair lineages. Thus, we propose a role for Med1 in safeguarding lineage specific enhancers, highlight the central role of enhancer accessibility and usage in lineage reprogramming and provide new insights into ectodermal regeneration.

INTRODUCTION

Postnatal cell fates are controlled by selective transcriptional programs, that are coordinated by an underlying epigenetic machinery and cellular microenvironments[1-4]. Ectoderm evolves into multiple lineages including enamel forming dental lineages, or to hair and epidermis generating skin epithelia[5-7]. Adult stem cells are endowed with tissue specific potential maintaining however the ability to differentiate into different cell types[8-10]To date, the mechanisms controlling specific cell lineage are yet not fully understood, and accordingly, the factors safeguarding dental or epidermal cell lineages are still largely elusive. Understanding these mechanisms is also crucial for our efforts in combating diseases like alopecia or tooth loss as it might create new entry points for the development of bioengineering strategies for the regeneration of tissues like tooth enamel and skin hair, which have been challenging[7].

The mouse incisor provides an excellent model system to study postnatal lineage commitment and progression. Dental epithelial stem cells (DE-SCs) residing in the cervical loop (CL) at the proximal end of incisors support the continuous growth of the incisors throughout the lifespan of a mouse. They regenerate the enamel organ by giving rise to all the dental epithelia such as enamel matrix producing ameloblasts, Notch1 regulated stratum intermedium (SI) and others[11-16].

Skin epithelia derived from the same ectoderm are divided into the interfollicular epidermis and hair follicles during embryonic stages of skin formation[6]. Postnatally, hair follicle stem cells residing in the bulge region of hair follicles regenerate hair in skin[17,18]. Hair follicles are essential for hair growth and regeneration in mammalian skin and are characterized by a complex multilayered bulb structure containing the outer and inner root

73 sheath, medulla, and cortex[19,20]. Following the initial developmental cycle, hair is
74 maintained by hair follicle cycling in mice, characterized by an anagen phase during which
75 the hair follicle expands, followed by a transitional catagen phase, leading to the involution
76 of the hair follicle, and telogen, the resting phase. The cycle then begins a new in
77 response to signals from the dermal papilla, a specialized mesenchymal group of cells
78 attached to the proximal end of the hair bulb[21,22]. The shift between these phases involves
79 substantial changes in gene expression patterns, which can be activated by injury. For
80 example, hair depilation induces new hair growth by stimulating anagen with induction of
81 gene expression such as those encoding hair keratins[23].

82 Several transcription factors and pathways have been shown to induce dental as
83 well as hair and epidermal cell differentiation. During embryonic development, dental and
84 skin epithelia share similar transcriptional networks as they are derived from the same
85 ectoderm. Postnatally, each lineage is controlled by specific transcription factors. For
86 example, paired like homeodomain 2 (*Pitx2)*[24] and Nk homeobox 3 (*Nkx2-3)*[25] ISL LIM
87 homeobox 1 (*Isl1)*[26] are implicated in enamel epithelial homeostasis[7] while transcription
88 factors and signaling genes including HR lysine demethylase and nuclear receptor
89 corepressor (*Hr also called hairless*) and Ras and Rab interactor 2 (*Rin2*) are important
90 in controlling hair differentiation because their mutation causes alopecia (hair loss)[27,28].
91 On the other hand, AP1 factors (*Fos/Jun*) and the tumor proteins of the p53 family
92 including *Tp63* are crucial to direct postnatal epidermal differentiation in the skin[20].
93 However, the check point factors specifying dental vs epidermal cell fate are still largely
94 elusive.

95 Mediator is a promising candidate to specify the ectodermal lineages. Mediator
96 complex controls cell lineages by facilitating the expression of cell fate driving
97 transcription factors and genes through large cluster of enhancers called super-
98 enhancers, that differs from typical enhancers in size and an ability to induce transcription
99 of cell identity genes[4,29]. Mediator 1 (Med1) is a subunit of the Mediator complex, which
100 facilitates gene transcription by linking enhancers to the RNA polymerase complex at
101 transcriptional start sites (TSS) in gene promoters. Med1 has been shown to localize at
102 super-enhancers and typical enhancers which represent distal regulatory elements
103 recognized as key epigenetic hubs[4,29]. In fact, Med1 assures pluripotency of embryonic
104 stem (ES) cells by enforcing the expression of Klf4, Oct4, Sox2, and Nanog, four key
105 reprogramming factors. In addition, reduced expression of Mediator subunit like *Med1*
106 triggers differentiation of ES cells[4,29]. Deletion of *Med1* also affects somatic cell fates such
107 as epidermal cells in skin[30-34]. *Med1* ablation hinders invariant natural killer T cell
108 development[35] and prevents luminal cell maturation in the mammary epithelia in mice[36,37].
109 These data indicate a role for *Med1* in controlling lineage commitment in somatic cells as
110 well. However, the exact role of *Med1* is not fully understood as previous biochemical
111 studies indicated that removal of Med1 disturbs selective transcription[38], but is
112 dispensable for Mediator complex formation[38].

113 In the present study, we investigate the role of *Med1* in governing ectoderm
114 lineages using a conditional knockout (cKO) mouse model, in which *Med1* expression is
115 deleted from ectoderm derived epithelial cells. *Med1* ablation causes hair generation in
116 incisors with loss of the ability of dental epithelia to produce enamel resulting in severe
117 enamel dysplasia[33,39,40]. Here, we present a unique cellular process by which *Med1*

118 ablation causes ectopic hair growth on incisors. Using an integrative multi-omics
119 approach, we also demonstrate that this intriguing phenomenon is due to a reshape of
120 the enhancer landscape in which ectoderm conserved enhancers are amplified to induce
121 epidermal and hair driving transcription factors.
122

123 **RESULTS**
124

125 **Lack of *Med1* in dental epithelia causes ectopic hair without hair follicles on**
126 **incisors.**

127 During postnatal murine tooth maintenance, CL residing dental epithelial stem cells (DE-
128 SCs) differentiate into Notch1 regulated SI, ameloblasts and other epithelia to mineralize
129 enamel on the incisor surface (Fig. 1a, top). Intriguingly, deletion of *Med1* from *Krt14*
130 expressing DE-SCs and their progenies provoked a major phenotypical shift in the dental
131 compartment causing enamel formation to be replaced by unusual, ectopic hair growth
132 on mouse incisors (Fig. 1b)[33]. As hair growth on the skin depends on multiple cell
133 populations arranged to form hair follicles (Fig. 1a, bottom), the question arises on how
134 hair development is achieved in a dental environment. Therefore, we evaluated the
135 cellular process leading to hair development in *Med1* cKO incisors by comparing it with
136 physiological hair in skin. Although hair grown on incisors of our mouse model showed a
137 comparable hair architecture (cuticle), composition (guard hair and zig-zag hair) and
138 morphology as naturally grown skin hair (Fig. 1b), hair formation significantly differed on
139 incisors in which hair supporting tissues and root structures lacked hair follicles (Fig. 1b
140 black follicles). In fact, while skin grown hair is regenerated from large anagen follicles in
141 response to signals from the dermal papilla and maintained by small telogen follicles (Fig.

142 1c, bottom orange arrows), we found that dental hair is supported by atypical cell clusters
143 without typical hair follicle-like structures in *Med1* cKO incisors at 4wk when hairs were
144 first visible (Fig. 1c Top, blue arrows with dotted lined region, and Suppl. Fig. 1e). These
145 abnormal cell clusters originated from disorganized SI layer (Suppl. Fig. 1b red triangles)
146 that progressed into expanded papillary layers (Suppl. Fig. 1c yellow triangles) to form
147 the hair bases in dental mesenchymal tissues (Suppl. Fig. 1e yellow triangles). NOTCH1
148 positive SI/SR derived papillary cells formed unusual cell aggregates and differentiated
149 into hair lineage as they express the hair marker keratin 71 (KRT71) at 4wk at maturation
150 stage (Suppl. Fig. 1d). At the adult stages (3 months of age and later), these aggregates
151 formed aberrant pocket-like structures (Fig. 2a). These NOTCH1 expressing SI/SR
152 derived cell clusters gave rise to hair KRT71 expressing cells as well as in cells
153 expressing the epidermal marker Loricrin (LOR) at 3 months of age (Fig. 2a, b). However,
154 the spatial organization of these cells was scattered and randomly distributed (Fig. 2b two
155 left panels, large blue arrows), that differed from the well-defined cellular framework found
156 along hair follicles and on the surface of the interfollicular epidermis in the skin (Fig. 2b,
157 right panels, orange arrows). Furthermore, hair depilation of skin initiated the hair cycle
158 by enlarging hair follicles (anagen) (Fig. 2c left 3 panels, orange arrows) and inducing the
159 expression of *Krt31* (Suppl. Fig. 2a skin). In contrast, dental hair depilation did not activate
160 any follicle-like structures in the hair supporting tissues on *Med1* null incisors (Fig. 2c two
161 right panels, blue arrows), in either distal or proximal incisor regions (Suppl. Fig. 2b) nor
162 is the expression of the hair marker *Krt31* induced (Suppl. Fig. 2a tooth). Nevertheless,
163 hair grew back at its original length 12 days after depilation in *Med1* cKO incisors (Fig. 2d
164 blue arrow), as occurred in normal skin (Suppl. Fig. 2c).

165 These results demonstrate that hair can grow and is regenerated through SI
166 derived dental epithelia even in the absence of well-organized hair follicle structural
167 features (Fig. 2e). Expression of hair and epidermal markers in the hair generating cell
168 aggregates further indicates that the presence of certain transcriptional patterns allow for
169 the generation of hair via a primitive cellular environment.

170 ***Med1* deficiency is sufficient to switch the dental transcriptional program towards**
171 **hair and epidermis in incisors *in vivo*.**

172 Cell identity and cell lineage progression tightly associate with a timed expression of
173 specific gene-sets. As loss of *Med1* causes hair growth in the dental compartment, using
174 total gene expression datasets we investigated the expression patterns of epidermal and
175 hair related gene sets at distinct anatomical locations of mouse incisors in *Med1* cKO
176 incisor (Fig. 3a, diagram). Our analyses revealed that compared to control mice, in *Med1*
177 cKO mice some epidermal genes are already induced in the DE-SCs containing CL region
178 at 4 weeks of age (Fig. 3b left panel, blue dotted box, Fig. 3c pale blue bar). Subsequently,
179 as DE-SCs differentiate towards the secretory (Sec) and maturation (Mat) stages,
180 expression of many epidermal genes strongly increased in *Med1* deficient tissue (Fig. 3b).
181 Intriguingly, hair related genes were not yet detected in the CL locus but become clearly
182 upregulated downstream in the Sec and Mat regions (Fig. 3b right panel, Fig. 3C blue
183 bar). Immunostaining confirmed the sequential induction of epidermal and hair markers
184 as the epidermal markers LOR and KRT1 were detected at secretory stage[39] but KRT71
185 was expressed only at maturation stage (Suppl, Fig. 1d). These data illustrate how in cKO
186 mice the expression of selected gene-sets during dental hair development parallels
187 embryonic and postnatal skin development in wild type mice where epidermal

188 development occurs first (E15) (Fig. 3c red bar), followed by hair follicle formation (E18)
189 (Fig. 3c orange bar). These results demonstrate that *Med1* deficiency is sufficient to
190 implement epidermal and hair related transcriptional programs priming dental stem cells
191 towards skin epithelial differentiation *in vivo*.

192 ***Med1* deletion redirects dental epithelial stem cells towards an epidermal fate in**
193 ***vitro*.**

194 Although deletion of *Med1* causes a lineage shift *in vivo*, the question arises if aberrant
195 dental hair growth is due to lineage predisposition of dental epithelial stem cells. To
196 investigate this phenomenon, dental stem cells from CL tissues were cultured. CL tissues
197 from 8-10 weeks old control and *Med1* cKO mice were micro-dissected and digested cells
198 were plated until self-renewing stem cell colonies formed (Fig. 4a, b). An enhanced
199 proliferation rate was observed for the *Med1* deficient cells as shown by the increased
200 number of BrdU positive cells as well as by the generation of larger colonies (Fig. 4b,
201 cKO). Confirming and expanding these results, IPA (ingenuity pathway analysis) of whole
202 transcriptomic data from these cultures not only revealed an upregulation of cell growth
203 and proliferation related pathways in *Med1* null cells, but also showed that these cells
204 spontaneously differentiate into the epidermal lineage in monolayer culture (Fig. 4c, d),
205 even without factors or mesenchymal feeder cells to induce epidermal differentiation. In
206 fact, like Sec tissue from cKO mice (Fig 4d middle column), an extensive set of epidermal
207 related genes are clearly upregulated in cultured *Med1* null DE-SCs as well (Fig. 4d right
208 column). Of note, in contrast to our *in vivo* data shown above, genes related to hair
209 differentiation are only partially induced *in vitro* (Fig. 4d), suggesting that full hair
210 differentiation requires additional external processes. Furthermore, IPA analysis also

211 identified members of the p53 family (Tp63/53/73) as top upstream inducers of epidermal
212 differentiation (Fig. 4e) that are linked to the key epidermal AP-1 transcription factors *Fos*
213 and *Jun* (Fig. 4f), resembling their roles in the skin. Collectively, these results show that
214 Med1 deletion reprograms DE-SCs towards epidermal fates through a cell intrinsic
215 mechanism. Together with our *in vivo* observation in *Med1* cKO, these results lead us to
216 investigate the underlying epigenetic and transcriptional mechanism, by which Med1
217 assures enamel lineage and Med1 deficiency causes a lineage shift.

218 **Med1 regulates enamel lineage driving transcription factors through super-**
219 **enhancers.**

220 Lineage commitment and reprogramming are controlled by cell fate driven transcription
221 factors. Mediator including Med1 orchestrates these key factors by associating with
222 super-enhancers and promoters[29]. Therefore, we first identified these key transcription
223 factors by assessing the genome wide distribution of MED1 containing enhancers during
224 dental epithelial development in control mice (4wk). For this purpose, we performed
225 MED1 ChIP-seq of the stem cell containing head region of the CL (CLH) as well as on
226 the CL tail area (CLT) which includes their progenies (Fig. 5a, left diagram). MED1
227 accumulated in the distal intergenic regions (Suppl. Fig. 3a) where it associated to several
228 hundred super-enhancers in the CLH and CLT tissues (Fig. 5b and Suppl. Fig. 3b). These
229 include super-enhancers near lineage driving transcription factors. In the CLH tissues,
230 these include enamel lineage transcription factors including *Pitx2*, *Isl1, and Nkx2-3* (Fig.
231 5b left panel and Fig. 5c left 3 panels), which may prime adult stem cells to an enamel
232 fate, consistent with their essential roles in tooth morphogenesis during embryonic
233 development[25,41]. In contrast, in CLT samples, MED1 super-enhancers were found

234 around key transcription factors like Satb1 homeobox 1 (*Satb1)* and Runx family
235 transcription factor 1 (*Runx1*) and 2 (*Runx2*) which control later cellular processes like
236 differentiation and enamel mineralization[41,42 43](Fig. 5b right pane and Fig. 5c right 3
237 panels). Of note, the mRNA expression levels of these transcription factors were strongly
238 reduced in CLT tissues in *Med1* cKO mice (Fig. 5d), further implicating their role in enamel
239 formation as *Med1* null mice show severe enamel dysplasia[40]. In addition, MED1 levels
240 are enriched around the promoters of these transcription factors but not of ameloblast
241 markers (Suppl Fig. 3d), indicating that Med1 directly activates enamel fate related
242 transcription factors rather than supporting late differentiation. These data indicate that
243 Med1 programs dental stem cells and their progenies to commit to and progress the
244 enamel lineage by controlling the expression of lineage driven transcription factors (Fig.
245 5e).

246 Intriguingly, we also found enhancers around a different set of transcription factors
247 (Suppl. Fig. 3c pink labeled) involved in epidermal differentiation of the skin including the
248 genes of early growth response (*Egr3)*, CCAAT enhancer binding protein β (*Cebpb*), Fos
249 like 2 (*Fosl2*) (AP-1 transcription factor subunit), Kruppel like factor 3 (*Klf3*), Forkhead box
250 C1 (*Foxc1*), *Foxo3*, tumor protein *Tp63*, and hair fate driving factors like *Hr* and *Rin2.*
251 Their mRNA expressions were substantially upregulated in *Med1* cKO mice at CLT
252 tissues (Fig. 5f), implicating their roles to induce epidermal and hair fates in *Med1* cKO
253 mice.

254 **Med1 deficiency reshapes the enhancer landscape in DE-SCs and their progenies.**
255 As loss of *Med1* inhibits the expression of Med1 associated enamel lineage driving
256 transcription factors while inducing epidermal transcription factors in CL tissues, we next

257 probed if this is linked to epigenetic changes in promoter and enhancer patterns upon
258 loss of *Med1*. To test this hypothesis, we performed ChIP-Seq analysis against an
259 alternative enhancer marker, histone 3 lysine 27 acetylation (H3K27ac), in CLH and CLT
260 tissues of 4-wk-old *Med1* cKO mice and their littermate controls (Fig. 6a) as the Med1
261 antibody is not useful for *Med1* cKO tissues. It is known that histone acetylation
262 (H3K27ac) generally co-localizes with Mediator such as Med1 at distal regulatory
263 elements like typical and super-enhancers and acts as a major inducer of gene
264 expression by increasing chromatin accessibility[29,44]. Compared to controls, we found
265 major genomic changes in the H3K27ac binding patterns of *Med1* cKO CLT tissues.
266 These were associated with biological functions such as enamel mineralization and tooth
267 morphogenesis (Fig. 6b blue bars), as well as epidermal and hair development (yellow
268 bars), consistent with the observed *Med1* cKO phenotypes. These results suggest that
269 phenotypic and transcriptional changes are due to epigenetic changes. In addition, *Med1*
270 deletion substantially increases the number of super-enhancers (Fig. 6c) as well as typical
271 enhancers (Suppl Fig. 4a) in both CLH and CLT. Some of these new enhancers are found
272 around loci coding for epidermal and hair lineage genes (Fig. 6c bar graphs) that become
273 upregulated upon loss of *Med1* in CLT tissue. For example, a new super-enhancer was
274 formed in the *Med1* cKO on epidermal transcription factor *Fosl2* (Ap-1 factor) loci (Fig. 6d
275 blue bar in boxed region), directly linking its increased mRNA expression to the loss of
276 *Med1* (see Fig. 5f and Suppl Fig. 4b). Corroborating these results and in line with our
277 transcriptional network studies in *Med1* null cell cultures (see Fig. 4f), we also found that
278 the binding motifs for the epidermal inducible transcription factors, Tp53/63, Egr1 and AP-
279 1 are significantly enriched in super-enhancers in cKO at CLT compared to controls (Fig.

280 6e). Collectively, these data demonstrate that loss of *Med1* alters the epigenetic
281 landscapes in DE-SCs and their progenies. These results prompted us to investigate the
282 epigenetic mechanism by which Med1 deficiency induces epidermal and hair lineages
283 more in detail.

284 ***Med1* deficiency induces epidermal and hair driving transcription factors via**
285 **amplification of ectoderm conserved enhancers.**

286 During embryonic development, dental and skin epithelia are derived from the same
287 ectoderm by sharing transcriptional networks. Our results indicated that normal dental
288 epithelia already possess enhancers around key epidermal and hair transcription factors
289 (Suppl Fig. 3c pink labeled). We further found that even though dental epithelia usually
290 do not commit to epidermal fates, they widely share the enhancers with skin epithelia both
291 epidermis and hair follicle derived cells[45] for most of the transcription factors induced upon
292 *Med1* loss (Fig. 7a). Importantly, *Med1* deficiency elevated and upgraded these shared
293 enhancers into transcriptionally active super-enhancers as outlined for the *Hr* (hairless)
294 locus (Fig. 7b pink bar and Suppl Fig. 4c). Loss of *Med1* also expanded enhancers in size
295 for epidermal factors *Cebpb* and *Foxo3* loci (Suppl. Fig 4d). In addition, enhancers near
296 many hair-lineage related genes were elevated to super-enhancers upon the loss of *Med1*
297 in CLT (Fig. 7c and Suppl. Fig. 4e) which coincided with an induction at their mRNA levels
298 that were measured by RNA-seq (Fig. 7d and Suppl. Fig. 5a). Intriguingly, these factors
299 controlling hair lineage were shown to be regulated by super-enhancers in the skin
300 before[4]. Besides the generation of new super-enhancers, we also found an increase in
301 H3K27ac levels around promoters of these genes (Suppl. Fig. 4f), which further positively
302 corelated with an increased gene expression (Fig. 7e). In *Med1* cKO CLH tissues,

303 increased H3K27ac promoter levels positively correlated with an elevated expression of
304 genes involved in preventing ossification (Suppl. Fig. 5a, and 6b, c), and H3K27ac
305 occupancy increased in ossification inhibiting transcription factors of *Sox9* and *Tob1* loci
306 in their enhancers (Suppl. Fig. 6c). This further corroborates the dental phenotype of our
307 mouse model which is not only characterized by hair growth but also by enamel dysplasia.
308 These results demonstrated that cell fate switch is at least in part due to an inflation of
309 developmentally conserved epidermal and hair enhancers.

310 In summary, we propose an epigenetic model in which *Med1* safeguards enamel
311 lineage commitment and progression of dental stem cells and their progenies. *Med1*
312 deletion shifts dental stem cells to epidermal fates by amplifying the ectodermal
313 conserved enhancers around hair and epidermal genes.

314

315 **DISCUSSION**

316

317 Adult stem cell fate is heavily linked to their tissue of origin[2,3,46]. It is postulated that the
318 local cellular and endocrine microenvironment primes and directs tissue specific lineage
319 commitment and differentiation via cellular, transcription and epigenetic mechanisms[2,4].
320 Here we show that deletion of *Med1*, a key component of enhancer associated Mediator
321 complex, causes ectopic hair growth on incisors. Unlike hair growth in the skin which
322 relies on functionally structured follicles, dental hair is generated from primitive, cellular
323 aggregates without hair follicle morphogenesis. Furthermore, as shown by our depilation
324 experiments, dental hair regrows without induction of the hair cycle, a follicle dependent
325 process required for regeneration of hair in the skin. Thus, our results question the current
326 knowledge that mammalian hair can only be generated from hair follicles consisting of

327 multiple cell layers bearing defined functions. In addition, our study also illustrates how
328 deletion of *Med1* induces lineage shift *in vivo*. Despite cellular agglomerates causing hair
329 growth on incisors exhibit a scattered cellular setup, the mRNA expression profiles found
330 in these structures mimic those of dedicated hair and epidermal cells found in skin
331 epithelia. Thus, while *Med1* negative DE-SCs reside in the dental environment, they are
332 driven towards lineages characteristic for skin epithelia.

333 Lineage commitment and differentiation are orchestrated by epigenetic programs
334 and regulatory elements including transcription factors and enhancers[4,29,44]. Our results
335 elucidate that already at early dental differentiation stages MED1 containing super-
336 enhancers selectively populate genomic loci coding for enamel fate driven transcription
337 factors in DE-SCs and their progenies. This outlines how *Med1* controls and programs
338 enamel epithelia's differentiation at multiple stages as it primes DE-SCs towards the
339 dental lineage via activation of *Nkx2-3, Pitx2* and *Isl1* and calibrates lineage progression
340 of DE-SC progenies by regulating the expression of *Runx1/2* and *Satb1.* These findings
341 are consistent with previous studies that *Nkx2-3* controls cusp formation in embryonic
342 dental epithelia[25], and that *Nkx2-3, Pitx2 and Runx2* are essential for dental
343 development[24,25,41]*. Isl1* is required for patterning and mineralization of enamel[26], Runx2
344 for enamel mineralization [41,42], and *Satb1* for cell polarity and enamel matrix secretion in
345 amelogenesis[43].

346 Intriguingly, although MED1 is a well-recognized super-enhancer component, loss
347 of *Med1* in CL tissues does not compromise super-enhancer formation which is consistent
348 with previous observation[38], but significantly widens the genomic enhancer landscape
349 instead. In the dental setting, this does not increase the potency of DE-SCs but rather

350 drives these cells into epidermal linages. This coincides with a shift in the super-enhancer
351 profiles around loci coding for transcription factors like *Hr* (hairless) and *Rin2* which are
352 essential for hair formation[27,28] as well as *Egr1/3, CEBP/a*, *CEBP/b*, and *Fosl2* which
353 control epidermal differentiation in skin[47,48]. Furthermore, our data show that Tp63/53
354 binding sites are enriched in super-enhancers in *Med1* cKO mice. These are master
355 regulators for the development of stratified epithelia *in vivo*[20] and drive epidermal
356 differentiation *in vitro*. In fact, *Med1* null mice activate Tp63 driven epidermal
357 differentiation in the skin, resulting in an accumulation of epidermal markers and lipids in
358 upper hair follicle keratinocytes resulting in hair loss[33].

359 Building on our previous studies[39], these results elucidate a central role for Med1
360 in assuring enamel lineage. Our results also reveal that basal enhancers are already
361 present at hair and epidermis driving transcription factor loci in control dental epithelia
362 suggesting that a basal epigenetic memory granting multipotency is already established
363 in pre-occurring ectoderm during embryonic development. Consequently, Med1
364 guarantees adult stem cells to commit to enamel lineage by restricting super-enhancer
365 formation to lineage specific loci. In addition, as loss of *Med1* causes DE-SCs to
366 differentiate into a developmentally related lineage might indicate that reprogramming of
367 DE-SCs into lineages originating from the same germ layer (ectoderm) is easier than
368 overcoming more strict and embryonically set epigenetic barriers[29].

369 Hair and tooth are difficult organs to regenerate through pluripotent stem cells
370 based regenerative medicine since no clinical trials have been reported even after
371 extensive efforts[49]. A deep understanding of the cellular and epigenetic mechanisms
372 controlling these lineages and their reprogramming creates new entry points for the

373 development of strategies to combat hair and tooth related diseases. Our results establish
374 that hair formation is achievable in tissue outside of the skin, even without the presence
375 of hair follicles. Similarly, hair was also accidentally generated by DE-SCs transplanted
376 into renal capsules during an effort to regenerate enamel[50]. This suggests that hair could
377 be generated via genetically engineered cell clusters or organoids *in vitro* which might be
378 easier than traditional strategies and bypass time consuming re-programming processes.
379 This would be of great benefit as it would greatly simplify *in vitro* hair generation and allow
380 hair growth without hair follicles which are very challenging to regenerate[51]. Similarly,
381 enamel regeneration might also be feasible by using foreskin derived epidermal stem
382 cells. In fact, cultured epidermal stem cells derived from skin have been shown to
383 differentiate into functional ameloblasts *in vitro*[52]. Overall, these findings, elucidate novel
384 possibilities to develop strategies to overcome hair and enamel associated diseases.
385

386 **MATERIALS AND METHODS**

387

388 **Krt14-driven *Med1* cKO mice**

389 Conditional *Med1* knockout (cKO) mice were generated as described previoulsy[33]. Floxed
390 (exon 8-10) *Med1* mice[53] (C57/BL6 background) were mated with keratin 14 (*Krt14*)
391 promoter driven *Cre* recombinase mice (The Jackson Laboratory, C57/BL6 background).
392 Genotyping was performed by PCR as previously described[33] and *Cre* negative littermate
393 mice served as controls (Ctrl). All the experiments were approved by the Institutional
394 Animal Care and Ethics Committee at the San Francisco Department of Veterans Affairs
395 Medical Center.

396 **Dental epithelial stem cell (DE-SC) culture**

397 CL tissue was separated from 10 wk *Med1* cKO and Ctrl mice, and epithelial tissues were
398 separated and treated by dispase (5U/ml Stem Cell Technology) to separate
399 mesenchymal tissues. Epithelial tissues are further dissociated by accutase (Sigma
400 Milipore), and cells were plated under low density to generate colonies and maintained
401 with DMEM media supplemented with recombinant EGF 20 ng/ml (R&D), FGF 25 ng/ml
402 (R&D), 1X B27 supplement (Gibco). After 8 days of culture, number and size of colonies
403 are evaluated, and RNA is prepared for microarray.

404 **BrdU staining**

405 DE-SC are labeled by BrdU and stained by a BrdU staining kit (Abcam) by following
406 manufacturer's instruction.

407 **Chromatin immunoprecipitation**

408 Chromatin IP was performed by using the LowCell# ChIP kit (Diagenode) for H3K27ac,
409 and the iDeal ChIP-kit (Diagenode) for MED1 according to the manufacturer's protocols
410 with some modifications as described below. Dissected CLH or CLT tissues were cross-
411 linked with 1% paraformaldehyde for 8 min (H3K27ac) or for 15 min (MED1) and
412 subsequently quenched with 0.125M glycine. Epidermal keratinocytes containing stem
413 and their progenies were isolated from mouse skin were fixed with 1% paraformaldehyde
414 for 10 min. Chromatin was then sonicated with a Covaris S2200 ultra-sonicator (Covaris,
415 Inc.) to obtain DNA fragments with an average length of 300±50 bp. The fragment size
416 was verified with an Agilent 2100 Bioanalyzer (Agilent Technologies). Sheared chromatin

417 was thereafter immunoprecipitated with Protein A-coated magnetic beads (Diagenode)
418 preincubated with 4.5 μg/IP MED1 antibody (Bethyl A300-793A) or 3 μg/IP H3K27ac
419 antibody (ab4729, Abcam). Chromatin input samples were used as reference. Complexes
420 were then washed and eluted from the beads with washing buffer and crosslinks were
421 reversed by incubation with proteinase K at 65°C for 4 hours. Immunoprecipitated DNA
422 along with genomic DNA (Inputs) were purified using the IPure v2 kit (Diagenode). IP
423 efficiency was confirmed by qPCR using primers provided in the kits. Experiments were
424 carried out in duplicates. ChIP-Seq libraries were generated using the Accel-NGS 2S Plus
425 DNA library kits (Swift Sciences) and amplified by PCR for 11-13 cycles. High molecular
426 weight smear was removed in the library by right side size selection using SPRI beads
427 (Beckman Coulter). The libraries were quantified by Agilent 2100 Bioanalyzer with the
428 high sensitivity DNA assay and sequenced on an Illumina HiSeq 4000 (UCSF Center of
429 advanced technology) in a single strand 50 bp run.

430 **Next generation DNA sequence data analysis**

431 For RNA-Seq data analysis, raw reads were assessed for run quality using fastqc version
432 0.72 followed by alignment to reference genome (mm10) using RNA STAR Galaxy
433 version 2.6.0b-1 with default settings. Differential gene expression analysis was
434 performed using feature Counts Galaxy version 1.6.3 and DESeq2 Galaxy version
435 2.11.40.2. For ChIP-Seq data analysis, raw reads from MED1 or H3K27ac ChIP-seq
436 sequencing experiments were assessed for quality using fastqc version 0.72, followed by
437 mapping to reference genome (mm10) using BWA Galaxy version 0.7.15.1 with standard
438 settings. Pooled peak calling was performed with MACS2 callpeak version
439 2.1.0.20140616.0 using broad peak settings and a minimum FDR cutoff of 0.05. Raw-

440 files for available H3K27ac ChIP-Seq datasets in public from wildtype mice hair stem cell
441 progenies were downloaded from the NCBI-SRA database (SRR1573273, SRR1573274)
442 and analyzed as described above. To assess significantly different peak occupancy
443 between two experimental groups, peak files (MACS2) were analyzed with DiffBind
444 Galaxy version 2.6.6.4 or 2.10.0. Peak size and location were visualized with IGV version
445 2.3.92. MAYO using group auto-scale for comparable visualization of all shown groups.
446 Peak intensity around TSS (±10 kbp) as well as genomic peak distribution was assessed
447 with CEAS software (Version1.0.0, Cistrome, Liu Lab). Gene-ontology analysis for Med1
448 or H3K27ac distal intergenic cis-regulatory elements was performed using GREAT
449 version 3.0.0 (Bejerano Lab, Stanford). Super enhancer analysis was performed using
450 the ROSE package and the software NaviSE. Overlapping typical and super-enhancers
451 between the shown comparisons were assessed with Bedtools (version 2.29) using a
452 minimum overlap of 50%. Motif analysis (de novo and known) was performed using
453 HOMER software [32]. Curated gene-sets used for analyses in this study are provided
454 upon requests.

455 **Reproducibility and statistical analysis**

456 All the experiments using *Med1* cKO and littermate control mice (n=3) were repeated with
457 at least two litters, and reproducibility was confirmed. The experiments using cultured
458 dental epithelia were conducted in duplicates for microarray, and reproducibility was
459 confirmed. Histologic analyses were performed using 2 sections per mouse per each
460 group of cKO and Ctrl, and representative images are shown. Statistical significance was
461 calculated using software integrated methods or two-tailed unpaired Student's t-test. If

462 not differently noted, differences with a *p*-value of less than 0.05 were considered as
463 statistically significant.

464 **Data availability**
465
466 The array data were submitted to a public database (GEO/NCBI/NIH
467 http://www.ncbi.nlm.nih.gov/geo). Data for *Med1* cKO (4wk), are available with accession
468 numbers GSE50672, GSE50671, GSE50670, respectively under the super-series
469 GSE50673. We are pending of RNA-seq and ChIP-seq data submission.

470

471 **AUTHOR CONTRIBUTIONS**
472
473 Conceptualization: Y.O., R.T., K.Y., S.F., P.D., D.D.B; Methodology: Y.O., R.T., T.N.,
474 K.Y.; Investigation: Y.O., R.T., T.N., K.Y.; Writing-Original Draft: Y.O. Writing-Review &
475 Editing: R.T., Y.O., S.F., P.D., D.D.B; Funding Acquisition: D.D.B., Y.O., S.F., K.Y.,
476 Resources: R.T., K.Y., S.F., D.D.B., Y.O.

477
478 **DECLARATION OF INTERESTS**

479 The authors declare no competing interests.

480

481 **ACKNOWLEDGMENTS**

482 We thank Ms. Sun Hee Kim Wong for in maintaining the mice and technical assistance.
483 We are also grateful to L. Hu, C. Fong for technical support. We also thank Dr A. Van
484 Wijnen for epigenetic supports. This work was supported by the NIH grant R21 DE025357
485 (YO), R01 AR050023 (DDB), DOD grant CA110338 (DDB), VA Merit I01 BX003814-01
486 (DDB).

487

REFERENCES

1 Wabik, A. & Jones, P. H. Switching roles: the functional plasticity of adult tissue stem cells. *EMBO J* **34**, 1164-1179 (2015). https://doi.org:10.15252/embj.201490386

2 Garcia-Prat, L., Sousa-Victor, P. & Munoz-Canoves, P. Proteostatic and Metabolic Control of Stemness. *Cell Stem Cell* **20**, 593-608 (2017). https://doi.org:10.1016/j.stem.2017.04.011

3 Middendorp, S. *et al.* Adult stem cells in the small intestine are intrinsically programmed with their location-specific function. *Stem Cells* **32**, 1083-1091 (2014). https://doi.org:10.1002/stem.1655

4 Adam, R. C. *et al.* Pioneer factors govern super-enhancer dynamics in stem cell plasticity and lineage choice. *Nature* **521**, 366-370 (2015). https://doi.org:10.1038/nature14289

5 Kaltschmidt, B., Kaltschmidt, C. & Widera, D. Adult craniofacial stem cells: sources and relation to the neural crest. *Stem Cell Rev Rep* **8**, 658-671 (2012). https://doi.org:10.1007/s12015-011-9340-9

6 Jimenez-Rojo, L., Granchi, Z., Graf, D. & Mitsiadis, T. A. Stem Cell Fate Determination during Development and Regeneration of Ectodermal Organs. *Front Physiol* **3**, 107 (2012). https://doi.org:10.3389/fphys.2012.00107

7 Yoshizaki, K., Fukumoto, S., Bikle, D. D. & Oda, Y. Transcriptional Regulation of Dental Epithelial Cell Fate. *Int J Mol Sci* **21** (2020). https://doi.org:10.3390/ijms21238952

8 Manini, I. *et al.* Multi-potent progenitors in freshly isolated and cultured human mesenchymal stem cells: a comparison between adipose and dermal tissue. *Cell Tissue Res* **344**, 85-95 (2011). https://doi.org:10.1007/s00441-011-1139-0

9 Bianco, P. "Mesenchymal" stem cells. *Annu Rev Cell Dev Biol* **30**, 677-704 (2014). https://doi.org:10.1146/annurev-cellbio-100913-013132

10 Bianco, P., Robey, P. G. & Simmons, P. J. Mesenchymal stem cells: revisiting history, concepts, and assays. *Cell Stem Cell* **2**, 313-319 (2008). https://doi.org:10.1016/j.stem.2008.03.002

11 Wang, X. P. *et al.* An integrated gene regulatory network controls stem cell proliferation in teeth. *PLoS Biol* **5**, e159 (2007). https://doi.org:10.1371/journal.pbio.0050159

12 Klein, O. D. *et al.* An FGF signaling loop sustains the generation of differentiated progeny from stem cells in mouse incisors. *Development* **135**, 377-385 (2008). https://doi.org:10.1242/dev.015081

13 Mitsiadis, T. A. & Graf, D. Cell fate determination during tooth development and regeneration. *Birth Defects Res C Embryo Today* **87**, 199-211 (2009). https://doi.org:10.1002/bdrc.20160

14 Fuchs, E., Tumbar, T. & Guasch, G. Socializing with the neighbors: stem cells and their niche. *Cell* **116**, 769-778 (2004). https://doi.org:S0092867404002557 [pii]

15 Juuri, E. *et al.* Sox2 marks epithelial competence to generate teeth in mammals and reptiles. *Development* **140**, 1424-1432 (2013). https://doi.org:10.1242/dev.089599

16 Juuri, E. *et al.* Sox2+ stem cells contribute to all epithelial lineages of the tooth via Sfrp5+ progenitors. *Dev Cell* **23**, 317-328 (2012). https://doi.org:10.1016/j.devcel.2012.05.012

17 Morita, R. *et al.* Tracing the origin of hair follicle stem cells. *Nature* **594**, 547-552 (2021). https://doi.org:10.1038/s41586-021-03638-5

18 Gonzales, K. A. U. & Fuchs, E. Skin and Its Regenerative Powers: An Alliance between Stem Cells and Their Niche. *Dev Cell* **43**, 387-401 (2017). https://doi.org:10.1016/j.devcel.2017.10.001

19 Sundberg, J. P., Peters, E. M. & Paus, R. Analysis of hair follicles in mutant laboratory mice. *J Investig Dermatol Symp Proc* **10**, 264-270 (2005). https://doi.org:10.1111/j.1087-0024.2005.10126.x

537 20 Botchkarev, V. A. & Flores, E. R. p53/p63/p73 in the epidermis in health and disease. *Cold*
538 *Spring Harb Perspect Med* **4** (2014). https://doi.org:10.1101/cshperspect.a015248
539 21 Greco, V. *et al.* A two-step mechanism for stem cell activation during hair regeneration.
540 *Cell Stem Cell* **4**, 155-169 (2009). https://doi.org:10.1016/j.stem.2008.12.009
541 22 Alonso, L. & Fuchs, E. The hair cycle. *J Cell Sci* **119**, 391-393 (2006).
542 https://doi.org:10.1242/jcs.02793
543 23 Sakai, Y. & Demay, M. B. Evaluation of keratinocyte proliferation and differentiation in
544 vitamin D receptor knockout mice. *Endocrinology* **141**, 2043-2049 (2000).
545 24 Lin, C. R. *et al.* Pitx2 regulates lung asymmetry, cardiac positioning and pituitary and tooth
546 morphogenesis. *Nature* **401**, 279-282 (1999). https://doi.org:10.1038/45803
547 25 Han, X. *et al.* The transcription factor NKX2-3 mediates p21 expression and ectodysplasin-
548 A signaling in the enamel knot for cusp formation in tooth development. *J Biol Chem* **293**,
549 14572-14584 (2018). https://doi.org:10.1074/jbc.RA118.003373
550 26 Naveau, A. *et al.* Isl1 Controls Patterning and Mineralization of Enamel in the Continuously
551 Renewing Mouse Incisor. *J Bone Miner Res* **32**, 2219-2231 (2017).
552 https://doi.org:10.1002/jbmr.3202
553 27 Panteleyev, A. A., Paus, R., Ahmad, W., Sundberg, J. P. & Christiano, A. M. Molecular
554 and functional aspects of the hairless (hr) gene in laboratory rodents and humans. *Exp*
555 *Dermatol* **7**, 249-267 (1998). https://doi.org:10.1111/j.1600-0625.1998.tb00295.x-i1
556 28 Basel-Vanagaite, L. *et al.* RIN2 deficiency results in macrocephaly, alopecia, cutis laxa,
557 and scoliosis: MACS syndrome. *Am J Hum Genet* **85**, 254-263 (2009).
558 https://doi.org:10.1016/j.ajhg.2009.07.001
559 29 Whyte, W. A. *et al.* Master transcription factors and mediator establish super-enhancers
560 at key cell identity genes. *Cell* **153**, 307-319 (2013).
561 https://doi.org:10.1016/j.cell.2013.03.035
562 30 Malik, S. & Roeder, R. G. Dynamic regulation of pol II transcription by the mammalian
563 Mediator complex. *Trends Biochem Sci* **30**, 256-263 (2005). https://doi.org:S0968-
564 0004(05)00081-2 [pii]
565 10.1016/j.tibs.2005.03.009
566 31 Kornberg, R. D. Mediator and the mechanism of transcriptional activation. *Trends*
567 *Biochem Sci* **30**, 235-239 (2005).
568 32 Taatjes, D. J. The human Mediator complex: a versatile, genome-wide regulator of
569 transcription. *Trends Biochem Sci* **35**, 315-322 (2010). https://doi.org:S0968-
570 0004(10)00025-3 [pii]
571 10.1016/j.tibs.2010.02.004
572 33 Oda, Y. *et al.* Coactivator MED1 ablation in keratinocytes results in hair-cycling defects
573 and epidermal alterations. *J Invest Dermatol* **132**, 1075-1083 (2012).
574 https://doi.org:10.1038/jid.2011.430
575 34 Oda, Y., Chalkley, R. J., Burlingame, A. L. & Bikle, D. D. The transcriptional coactivator
576 DRIP/mediator complex is involved in vitamin D receptor function and regulates
577 keratinocyte proliferation and differentiation. *J Invest Dermatol* **130**, 2377-2388 (2010).
578 https://doi.org:10.1038/jid.2010.148
579 35 Yue, X., Izcue, A. & Borggrefe, T. Essential role of Mediator subunit Med1 in invariant
580 natural killer T-cell development. *Proc Natl Acad Sci U S A* **108**, 17105-17110 (2011).
581 https://doi.org:10.1073/pnas.1109095108
582 36 Jiang, P. *et al.* Key roles for MED1 LxxLL motifs in pubertal mammary gland development
583 and luminal-cell differentiation. *Proc Natl Acad Sci U S A* **107**, 6765-6770 (2010).
584 https://doi.org:10.1073/pnas.1001814107
585 37 Jia, Y. *et al.* Peroxisome proliferator-activated receptor-binding protein null mutation
586 results in defective mammary gland development. *J Biol Chem* **280**, 10766-10773 (2005).
587 https://doi.org:10.1074/jbc.M413331200

588 38 Zhang, X. *et al.* MED1/TRAP220 exists predominantly in a TRAP/ Mediator subpopulation
589 enriched in RNA polymerase II and is required for ER-mediated transcription. *Mol Cell* **19**,
590 89-100 (2005). https://doi.org:10.1016/j.molcel.2005.05.015
591 39 Yoshizaki, K. *et al.* Ablation of coactivator Med1 switches the cell fate of dental epithelia
592 to that generating hair. *PLoS One* **9**, e99991 (2014).
593 https://doi.org:10.1371/journal.pone.0099991
594 40 Yoshizaki, K. *et al.* Mediator 1 contributes to enamel mineralization as a coactivator for
595 Notch1 signaling and stimulates transcription of the alkaline phosphatase gene. *J Biol*
596 *Chem* **292**, 13531-13540 (2017). https://doi.org:10.1074/jbc.M117.780866
597 41 Xuan, D. *et al.* Effect of cleidocranial dysplasia-related novel mutation of RUNX2 on
598 characteristics of dental pulp cells and tooth development. *J Cell Biochem* **111**, 1473-1481
599 (2010). https://doi.org:10.1002/jcb.22875
600 42 Chu, Q. *et al.* Ablation of Runx2 in Ameloblasts Suppresses Enamel Maturation in Tooth
601 Development. *Sci Rep* **8**, 9594 (2018). https://doi.org:10.1038/s41598-018-27873-5
602 43 Zhang, Y. *et al.* SATB1 establishes ameloblast cell polarity and regulates directional
603 amelogenin secretion for enamel formation. *BMC Biol* **17**, 104 (2019).
604 https://doi.org:10.1186/s12915-019-0722-9
605 44 Hnisz, D. *et al.* Super-enhancers in the control of cell identity and disease. *Cell* **155**, 934-
606 947 (2013). https://doi.org:10.1016/j.cell.2013.09.053
607 45 Lien, W. H. *et al.* Genome-wide maps of histone modifications unwind in vivo chromatin
608 states of the hair follicle lineage. *Cell Stem Cell* **9**, 219-232 (2011).
609 https://doi.org:10.1016/j.stem.2011.07.015
610 46 Wei, Y. *et al.* Human skeletal muscle-derived stem cells retain stem cell properties after
611 expansion in myosphere culture. *Exp Cell Res* **317**, 1016-1027 (2011).
612 https://doi.org:10.1016/j.yexcr.2011.01.019
613 47 Kim, K. H. *et al.* EGR3 Is a Late Epidermal Differentiation Regulator that Establishes the
614 Skin-Specific Gene Network. *J Invest Dermatol* **139**, 615-625 (2019).
615 https://doi.org:10.1016/j.jid.2018.09.019
616 48 House, J. S., Zhu, S., Ranjan, R., Linder, K. & Smart, R. C. C/EBPalpha and C/EBPbeta
617 are required for Sebocyte differentiation and stratified squamous differentiation in adult
618 mouse skin. *PLoS One* **5**, e9837 (2010). https://doi.org:10.1371/journal.pone.0009837
619 49 Zhang, W. & Yelick, P. C. Tooth Repair and Regeneration: Potential of Dental Stem Cells.
620 *Trends Mol Med* **27**, 501-511 (2021). https://doi.org:10.1016/j.molmed.2021.02.005
621 50 Zheng, L. W., Linthicum, L., DenBesten, P. K. & Zhang, Y. The similarity between human
622 embryonic stem cell-derived epithelial cells and ameloblast-lineage cells. *Int J Oral Sci* **5**,
623 1-6 (2013). https://doi.org:10.1038/ijos.2013.14
624 51 Takeo, M. *et al.* Expansion and characterization of epithelial stem cells with potential for
625 cyclical hair regeneration. *Sci Rep* **11**, 1173 (2021). https://doi.org:10.1038/s41598-020-
626 80624-3
627 52 Hu, X. *et al.* Efficient induction of functional ameloblasts from human keratinocyte stem
628 cells. *Stem Cell Res Ther* **9**, 126 (2018). https://doi.org:10.1186/s13287-018-0822-4
629 53 Jia, Y. *et al.* Transcription coactivator PBP, the peroxisome proliferator-activated receptor
630 (PPAR)-binding protein, is required for PPARalpha-regulated gene expression in liver. *J*
631 *Biol Chem* **279**, 24427-24434 (2004). https://doi.org:10.1074/jbc.M402391200
632 M402391200 [pii]
633

634 **Figure legends**

635 **Fig. 1: Loss of *Med1* in dental stem cells causes ectopic hair growth on incisors. a**
636 Top**,** diagram representing normal dental epithelial differentiation and enamel formation
637 in mouse mandible. CL, cervical loop; Sec; secretory stage; Mat, maturation stage; DE-
638 SCs, dental epithelial stem cells; SI, stratum intermedium. Bottom, hair regeneration by
639 hair follicles under cycling regulation of anagen and telogen in skin. **b** Hair growth on
640 *Med1* cKO incisors at 4 weeks of age (top) is compared to normal hair in skin (bottom). **c**
641 Top, H&E sections of tissues supporting hair growth (blue arrows with dotted lines) in
642 *Med1* cKO incisors at 4 weeks of age. Bottom, H&E sections for hair follicles at anagen
643 and telogen phases supporting hair growth and regeneration in the skin (orange arrows).
644 Bars = 25 μm. For (**b, c**), representative images are shown.

645 **Fig. 2: *Med1* null incisors develop and regenerate hair without hair follicles. a** Left,
646 diagram depicting hair generation via pocket-like structures (red) in *Med1* cKO incisors in
647 adult mice. Right, H&E staining to evidence hair in dental tissues and immuno-staining
648 against hair marker KRT71 (green). **b** Top, immuno-staining of hair marker KRT71
649 (green) and NOTCH1 (red) in the aberrant pockets on *Med1* cKO incisors or of KRT71
650 only (green) in normal skin. Bottom, epidermal marker Lor (green) and NOTCH1 (red) in
651 dental tissues compared to Lor (green) and KRT14 (red) localization the skin. Small blue
652 arrows show auto-fluorescent hair structures. **c** H&E staining sections of skin (orange)
653 and dental (blue) sections before (day 0) and after hair depilation (3 and 7 days). Small
654 arrows show hair. Bars = 25 μm. **d** Full hair regeneration 12 days after hair depilation
655 from *Med1* cKO mice (blue arrow). **e** Schematic representation of cellular processes and
656 anatomical location of dental SI/SR derived dental epithelia that are gradually transformed

657 into epidermal (pale green) and hair gene expressing (green) aberrant cell aggregates
658 that lack hair follicle structures in *Med1* cKO incisors. For **a**-**d**, representative images are
659 shown, and reproducibility was confirmed at least in two different litters of *Med1* cKO and
660 control mice.

661 **Fig. 3: Loss of *Med1* activates epidermal and hair gene expression in developing**
662 **incisors. a** Diagram depicting the anatomical locations tested in Ctrl and *Med1* cKO
663 incisors. CL, cervical loop; Sec, secretory stage; Mat, maturation stage. **b** Heatmap
664 showing differential gene expressions for epidermal genes (left) and hair genes (right) in
665 *Med1* cKO incisors versus Ctrls at 4 weeks of age. For each gene, fold changes are
666 compared to CL Ctrl; n=3 for all samples and average values for each group are shown.
667 **c** Top, diagram depicts sequential expression of epidermal genes (light blue) and hair
668 genes (blue) as well as hair growth (purple) in *Med1* cKO mice in regard to the different
669 anatomical locations on incisors (CL, Sec and Mat) of *Med1* cKO incisors. Bottom, pattern
670 comparison to epidermal (orange, E15) and hair gene inductions (yellow, E18) during
671 embryonic development of the skin.

672 **Fig. 4: *Med1* deficiency directs DE-SCs towards epidermal fate *in vitro*. a** Generation
673 of DE-SC culture from CL tissues. **b** Left, representative bright field images of DE-SC
674 colonies and BrdU staining in Ctrl and *Med1* cKO. Bar = 10 μm. Right, quantification of
675 colony size and BrdU positive cells/colony are shown as fold changes (cKO/Ctrl); in both
676 comparisons $p>0.01$. **c** Biological processes associated with loss of *Med1* in DE-SCs as
677 identified by Ingenuity Pathway Analysis (IPA) on microarray gene expression data. **d**
678 Heatmap showing differential gene expressions of epidermal and hair related genes in
679 *Med1* cKO vs Ctrl incisor tissues (CL and Sec *in vivo*) and cultured *Med1* cKO vs Ctrl DE-

680 SCs (third lane); n=3 for all samples and average values for each comparison are shown.
681 **e** Upstream regulators responsible for biological process induced by loss of *Med1* in DE-
682 SCs as identified by IPA on microarray data as used in (**c**). **f** Mechanistic network
683 representation for TP53/63 pathways in induced in *Med1* lacking DE-SC culture
684 regulating epidermal fate driving AP-1 factors; upregulated genes are in orange and direct
685 relationships are shown by solid lines. Reproducibility was confirmed by two independent
686 cultures, and representative data are shown.

687 **Fig. 5: Med1 directly controls enamel lineage transcription factors by associating**
688 **with their enhancers and promoters. a** Schematic representation of tissues isolated
689 (CLH stem cells, and CLT their progenies) from normal mouse mandibles for MED1 Chip-
690 seq and RNA-seq. **b** MED1 bound enhancer clustering in CLH and CLT tissues. Light
691 gray and blue dots represent super-enhancers, dark grey dots are typical enhancers; blue
692 dots outline super-enhancer associated enamel transcription factors as designated by
693 gene name and enhancer ranking numbers. **c** Genomic MED1 binding profiles in CLH
694 (light blue) and CLT (blue) tissues for relevant transcription factors. Super-enhancers
695 (SE) are marked by bars with asterisks*. Average profiles from two independent Chip-seq
696 experiments are shown. **d** Transcription factors (TFs) identified through MED1 super-
697 enhancers that were down-regulated in *Med1 cKO* (CLT) as measured by RNA-seq. **e**
698 Schematic representation of Med1 to induce enamel fate transcription factors (TFs); distal
699 Med1 (red) containing super-enhancers associate to gene promoter to induce mRNA
700 expression (blue waves). **f** Enhancer associated epidermal or hair fate transcription
701 factors (TFs) that were upregulated in cKO (CLT) as measured by RNA-seq**. d, f** Data

702 are shown as average and SD of fold changes (log_2FC) in cKO compared to Ctrl within
703 two different litters of *Med1* cKO and control mice with statistical significance ($p<0.05$).
704 **Fig. 6: Loss of *Med1* expands the super-enhancer landscape in CLH and CLT**
705 **tissues. a** Schematic representation for the isolation of CLH (stem cells) and CLT (their
706 progenies) from *Med1* cKO and littermate Ctrl mandibles for Chip-seq against H3K27ac
707 to compare actively transcribed genomic regions. **b** GREAT based GO analysis for genes
708 associated with differential H3K27ac peaks to elucidate biological processes affected by
709 *Med1* loss in CLT tissues. **c** Number of super-enhancers in Ctrl (blue) and cKO (pink)
710 tissues. Bar charts comparing typical and super-enhancers associated with epidermal
711 and hair related genes before and after loss of *Med1* in CLH and CLT tissues. As a
712 comparison, data from skin derived keratinocytes are included. **d** Chip-seq profiles for
713 H3K27ac occupancy for *Fosl2* gene, in which the super-enhancer in cKO is marked by
714 blue line. **e** Most enriched transcription factor binding motifs found in super-enhancers
715 formed in *Med1* cKO compared to Ctrl in CLT tissues; statistical significance are shown
716 as log_{10}(*p*-values). All the Chip-seq data are average of duplicates conducted in 2 different
717 litters of *Med1* cKO and littermate controls.
718 **Fig. 7: Loss of *Med1* advances pre-existing enhancers to super-enhancers near**
719 **epidermal and hair lineage genes. a** Top, Schematic representations of cell sources of
720 dental and skin epithelia are shown. Bottom, heatmap showing shared enhancers
721 between dental and skin epithelia for epidermal and hair lineage related transcription
722 factors that are upregulated in *Med1* cKO. Shared enhancers in dental (CLH, CLT), and
723 skin epithelia including epidermal keratinocytes (Epi), and transient amplifying (TAC) hair
724 follicle keratinocytes (hair) are aligned. **b** Chip-seq profiles around the *Hr* (hairless) locus in

725 CLH and CLT from *Med1* cKO (pink) and Ctrl (blue) mice, compared to epidermal cells (green)
726 and hair TAC keratinocytes (light blue) from skin. Pre-existing enhancers in Ctrl (blue bar)
727 are develop into super-enhancers (pink bar) upon loss of *Med1* cKO in CLT. **c** Enhancer
728 distribution profiles; super-enhancers associated hair lineage genes and exclusively
729 found in Ctrl or *Med1* cKO CLT tissues are noted by the name of neighboring gene (blue
730 circles). **d** Heatmap depicting differential gene expression of hair lineage genes in *Med1*
731 cKO compared to Ctrl in CLT. **e** Correlation between gene expression and H3K27ac
732 promoter occupancy (TSS +/-30 kb) in *Med1* cKO vs Ctrl in CLT tissues for the hair
733 lineage driving gene set (orange dots) compared to all the other genes (blue dots). FC,
734 fold change.

Fig. 1

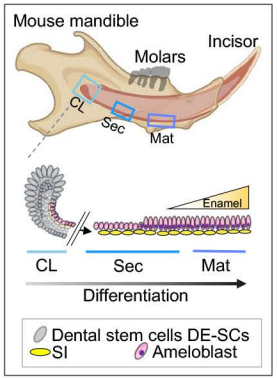
a
Mouse mandible
Incisor
Molars
CL
Sec
Mat
Enamel
CL
Sec
Mat
Differentiation
Dental stem cells DE-SCs
SI
Ameloblast

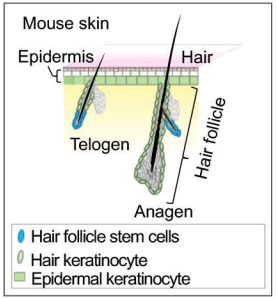
Mouse skin
Epidermis
Hair
Telogen
Hair follicle
Anagen
Hair follicle stem cells
Hair keratinocyte
Epidermal keratinocyte

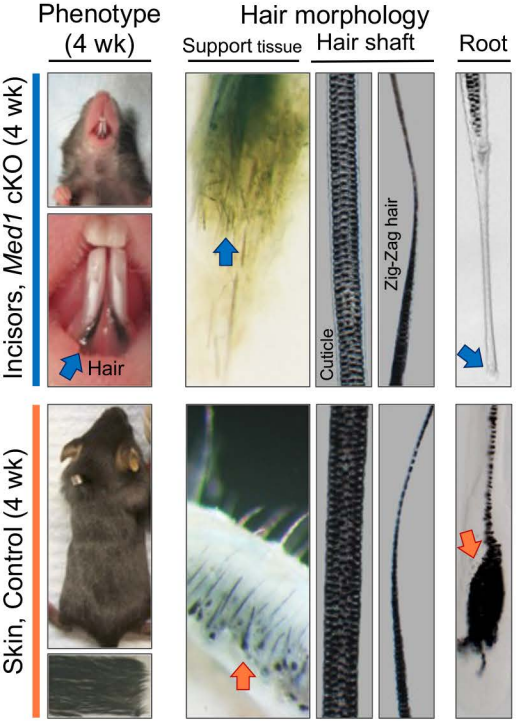
b
Phenotype (4 wk)
Hair morphology
Support tissue
Hair shaft
Root
Incisors, Med1 cKO (4 wk)
Hair
Cuticle
Zig-Zag hair
Skin, Control (4 wk)

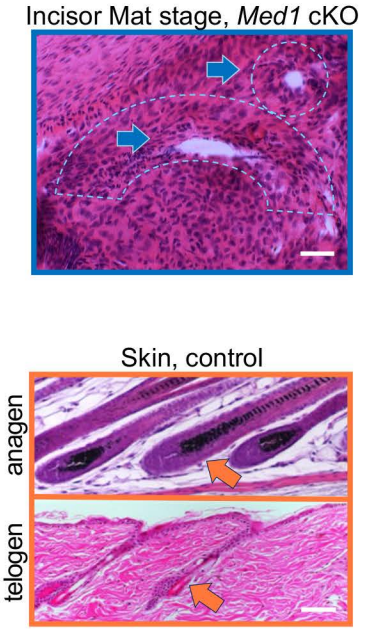
c
Incisor Mat stage, Med1 cKO
Skin, control
anagen
telogen

Fig. 2

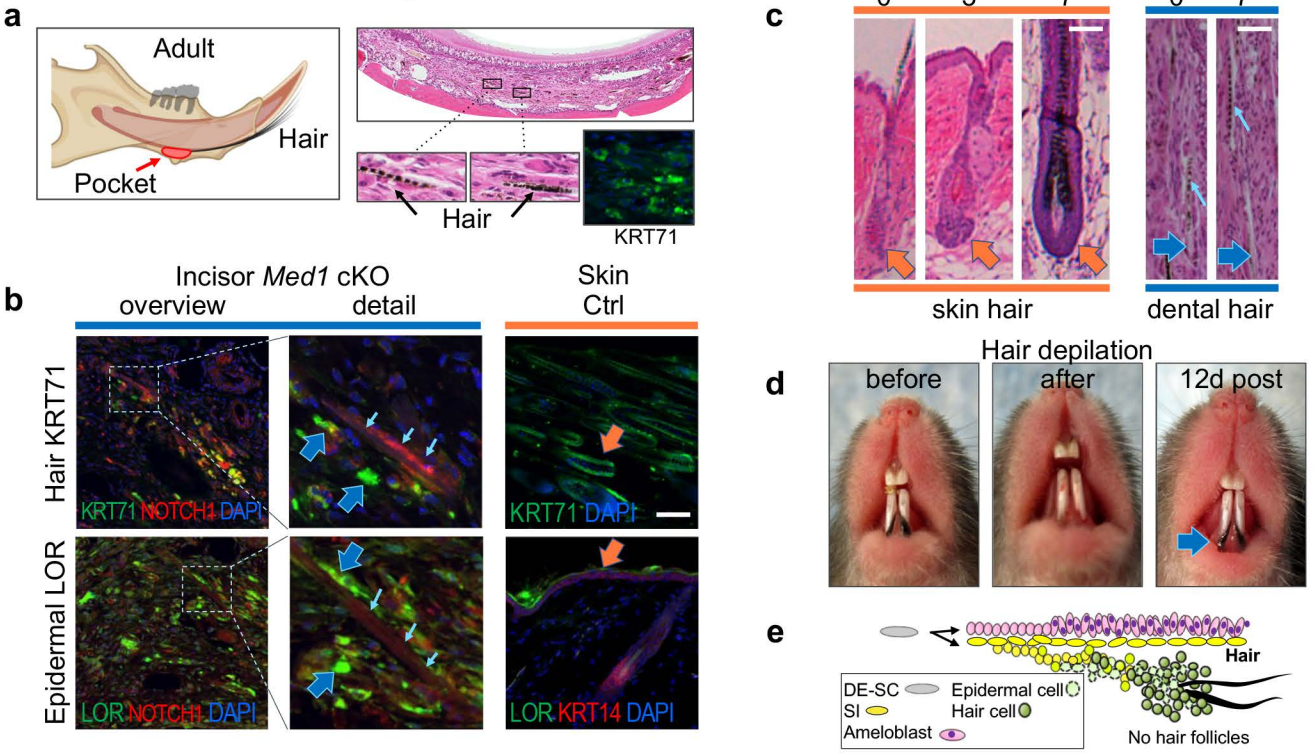
a
Adult
Hair
Pocket
Hair
KRT71
b
Incisor Med1 cKO
overview
detail
Skin
Ctrl
Hair KRT71
KRT71 NOTCH1 DAPI
KRT71 DAPI
Epidermal LOR
LOR NOTCH1 DAPI
LOR KRT14 DAPI
c
Days post depilation
0
3
7
0
7
skin hair
dental hair
d
Hair depilation
before
after
12d post
e
Hair
DE-SC
SI
Ameloblast
Epidermal cell
Hair cell
No hair follicles

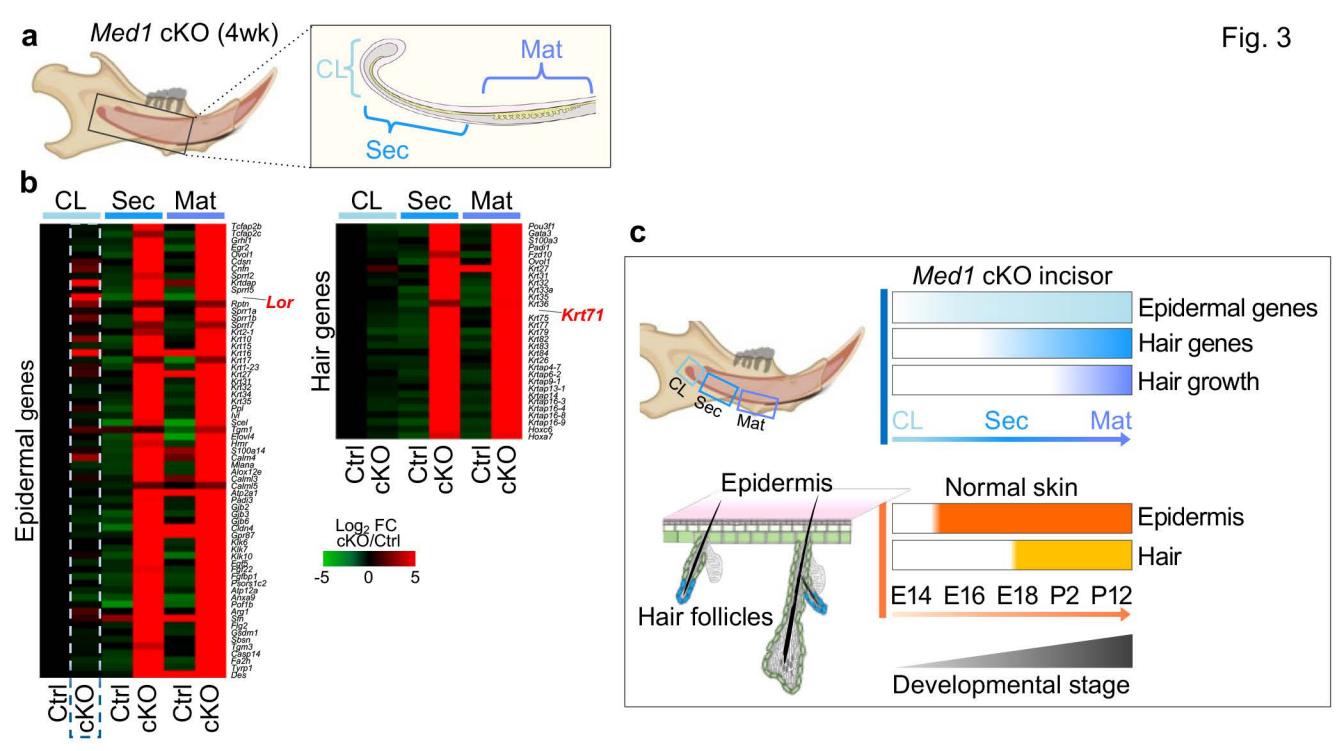

a
Med1 cKO (4wk)
CL
Mat
Sec
b
CL
Sec
Mat
Epidermal genes
Lor
Ctrl
cKO
Hair genes
Krt71
Log2 FC
cKO/Ctrl
-5
0
5
c
Med1 cKO incisor
Epidermal genes
Hair genes
Hair growth
Epidermis
Normal skin
Hair follicles
E14
E16
E18
P2
P12
Developmental stage

Fig. 3

Fig. 4

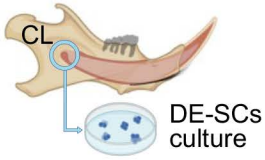

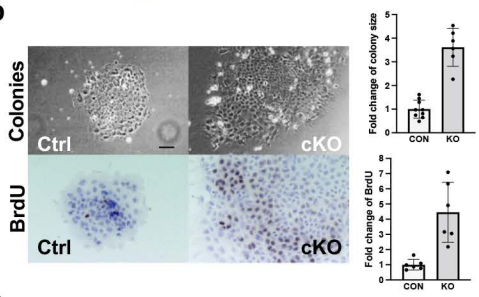

c

	p-values	#Molecules
Cellular growth and proliferation	6.03E-05 - 2.14E-30	611
Hair and skin development and function	4.97E-05 - 5.26E-18	119

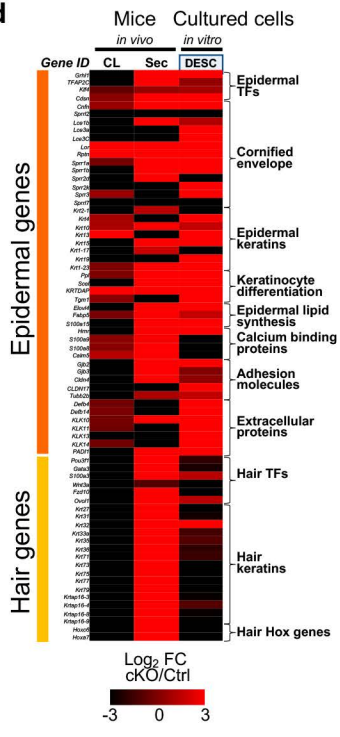

e

Upstream Regulator	Activation z-score	*p*-value
TP53	2.7	3.39E-25
TP63	0.2	1.93E-19
FOS	3.1	8.78E-19
TP73	0.7	4.98E-17
CEBPB	0.1	8.98E-15

f

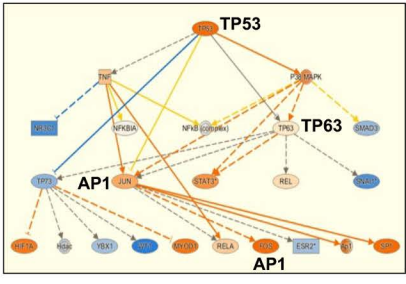

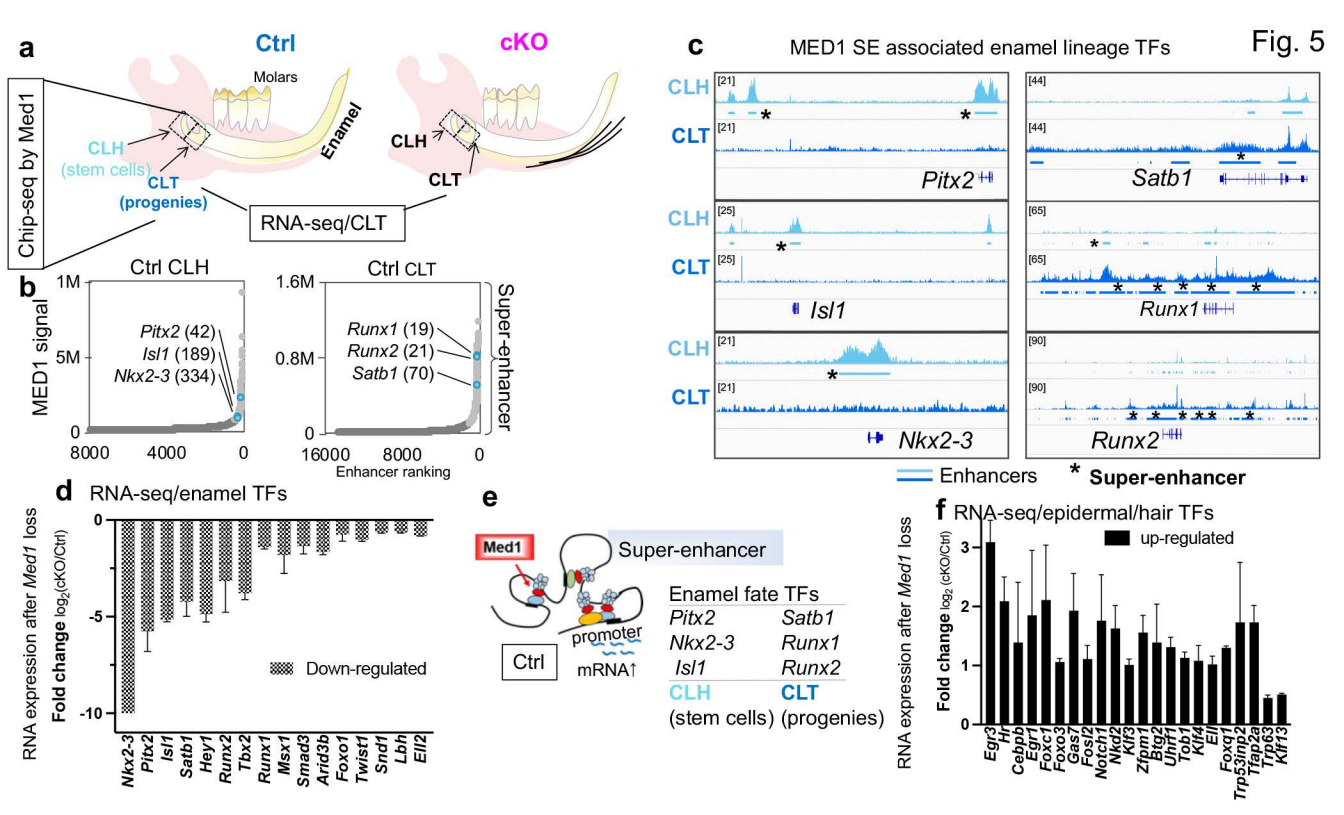
Fig. 5
a
Ctrl
cKO
Molars
Enamel
CLH
(stem cells)
CLT
(progenies)
Chip-seq by Med1
RNA-seq/CLT
b
Ctrl CLH
Ctrl CLT
MED1 signal
Pitx2 (42)
Isl1 (189)
Nkx2-3 (334)
Runx1 (19)
Runx2 (21)
Satb1 (70)
Super-enhancer
Enhancer ranking
c
MED1 SE associated enamel lineage TFs
Pitx2
Satb1
Isl1
Runx1
Nkx2-3
Runx2
Enhancers
Super-enhancer
d
RNA-seq/enamel TFs
RNA expression after Med1 loss
Fold change log2(cKO/Ctrl)
Down-regulated
Nkx2-3
Pitx2
Isl1
Satb1
Hey1
Runx2
Tbx2
Runx1
Msx1
Smad3
Arid3b
Foxo1
Twist1
Snd1
Lbh
Ell2
e
Med1
Super-enhancer
promoter
mRNA↑
Ctrl
Enamel fate TFs
Pitx2 Satb1
Nkx2-3 Runx1
Isl1 Runx2
CLH CLT
(stem cells) (progenies)
f
RNA-seq/epidermal/hair TFs
up-regulated
RNA expression after Med1 loss
Fold change log2(cKO/Ctrl)
Egr3
Hr
Cebpb
Egr1
Foxc1
Foxo3
Gas7
Fosl2
Notch1
Nkd2
Klf3
Zfpm1
Btg2
Uhrf1
Tob1
Klf4
Ell
Foxq1
Trp53inp2
Tfap2a
Trp63
Klf13

Fig. 6

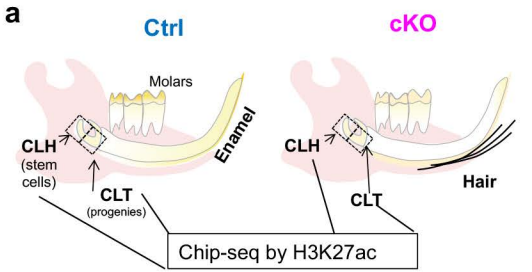

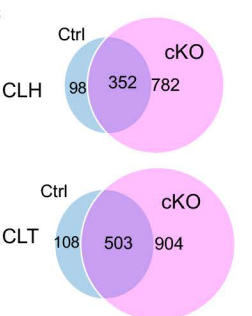

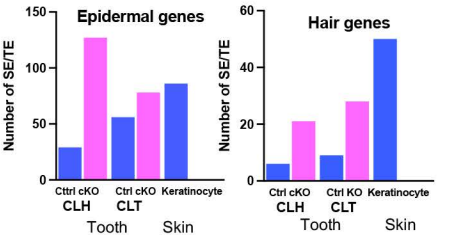

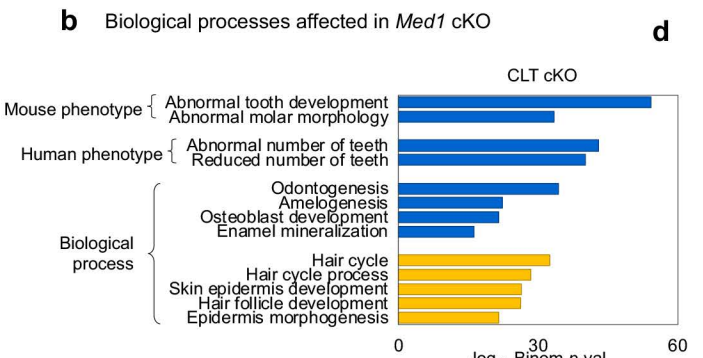

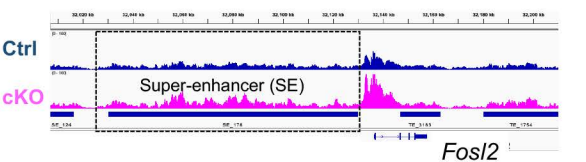

e

Name	Motif	-Log10 *p*-value Ctrl	-Log10 *p*-value cKO
p63/53		-2.1e+02	-8.0e+02
Egr1		-1.8e+02	-6.2e+02
AP-1		-1.7e+02	-6.5e+02

Fig. 7

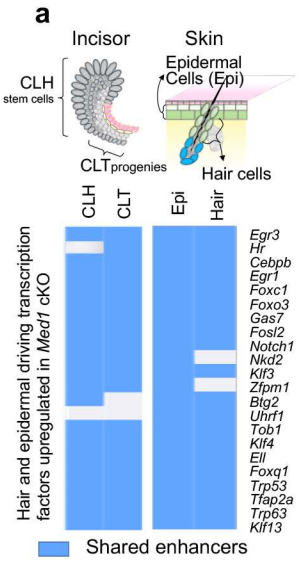
a
Incisor
Skin
CLH
stem cells
Epidermal
Cells (Epi)
CLT progenies
Hair cells
CLH
CLT
Epi
Hair
Hair and epidermal driving transcription factors upregulated in Med1 cKO
Egr3
Hr
Cebpb
Egr1
Foxc1
Foxo3
Gas7
Fosl2
Notch1
Nkd2
Klf3
Zfpm1
Btg2
Uhrf1
Tob1
Klf4
Ell
Foxq1
Trp53
Tfap2a
Trp63
Klf13
Shared enhancers

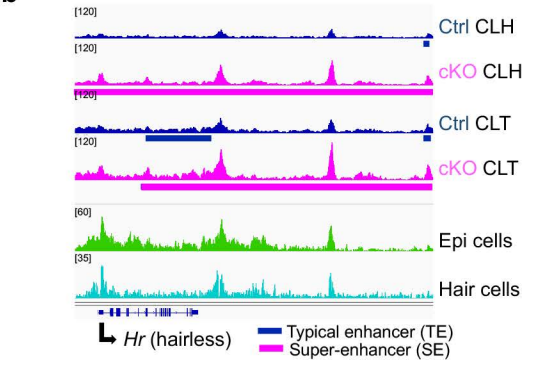
b
[120]
Ctrl CLH
[120]
cKO CLH
[120]
Ctrl CLT
[120]
cKO CLT
[60]
Epi cells
[35]
Hair cells
Hr (hairless)
Typical enhancer (TE)
Super-enhancer (SE)

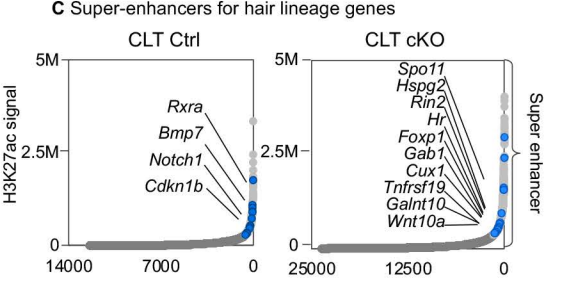
c Super-enhancers for hair lineage genes
CLT Ctrl
CLT cKO
H3K27ac signal
5M
2.5M
0
14000
7000
0
25000
12500
0
Rxra
Bmp7
Notch1
Cdkn1b
Spo11
Hspg2
Rin2
Hr
Foxp1
Gab1
Cux1
Tnfrsf19
Galnt10
Wnt10a
Super enhancer

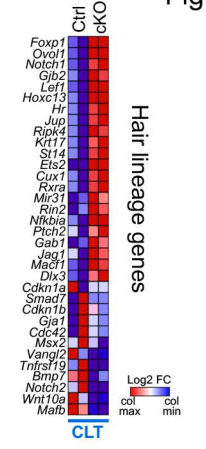
d
Ctrl
cKO
Foxp1
Ovol1
Notch1
Gjb2
Lef1
Hoxc13
Hr
Jup
Ripk4
Krt17
St14
Ets2
Cux1
Rxra
Mir31
Rin2
Nfkbia
Ptch2
Gab1
Jag1
Macf1
Dlx3
Cdkn1a
Smad7
Cdkn1b
Gja1
Cdc42
Msx2
Vangl2
Tnfrsf19
Bmp7
Notch2
Wnt10a
Mafb
Hair lineage genes
Log2 FC
col max
col min
CLT

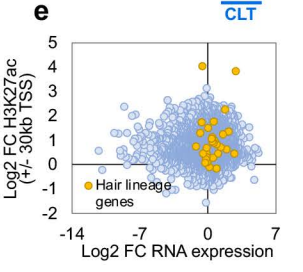
e
Log2 FC H3K27ac (+/- 30kb TSS)
5
4
3
2
1
0
-1
-2
-14
-7
0
7
Log2 FC RNA expression
Hair lineage genes

Supplemental information

Supplemental methods

Histological analysis

Mouse mandibles were dissected from *Med1* cKO and littermate control (Ctrl) mice and fixed in 4% paraformaldehyde at 4°C overnight and decalcified in 0.5 M EDTA for two weeks. Subsequently they were dehydrated and embedded in paraffin wax using standard protocols. The whole mandible was then serially sectioned at a thickness of 7 μm (sagittal sections) containing both the CL and enamel organ. Ultimately, slides were stained with hematoxylin and eosin (HE) and imaged with brightfield microscopy.

Immunostaining

For immunostaining, paraffin embedded jaw sections were treated with antigen unmasking solutions (Vector lab Citrate-based, H-3300) and subsequently blocked with an avidin/biotin blocking solution (Vector lab, SP-2001) and incubated with primary antibodies against Krt71 (Covance), Notch1 (Cell Signaling) and Loricrin (Covance). They were then developed with the Vectastain Elite ABC kit (Vector Lab) using DAB staining solution (Vector Lab, SK-4100) until brown signals were visible. The sections were counterstained with Gill's Hematoxylin.

Immunofluorescence

Paraffin-embedded mandible sections were pretreated in 10 mmol/L citrate buffer (pH 6.0, Sigma-Aldrich) for 20 min using a microwave for antigen retrieval. The specimens were blocked by Power Block (BioGenex) and incubated with primary antibodies against

KRT71 (Progen), KRT1, (Covance), LORICRIN (Covance) and NOTCH1 (Cell signaling). They were subsequently incubated with species specific secondary antibodies conjugated to fluorescent dyes (Invitrogen Molecular probes), including Alexa 594 (red) and Alexa 488 (green) and counterstained with DAPI. Images were taken with a confocal microscope (LSM510, Carl Zeiss).

RNA expression analysis

Total RNA was isolated from 4-week-old total CL, CLH, CLT, Sec or Mat tissues of *Med1* cKO and littermate Ctrl mice using the Pico Pure RNA purification kit (ABI). RNA from cultured dental epithelial stem cells was extracted using the RNeasy mini kit (Qiagen). RNAs were analyzed for quality and purity using the Pico Chip kit on an Agilent 2100 Bioanalyzer (Agilent Technologies) to meet the processing criteria of the UCLA Genomic Core facility for the Illumina array platform (Mouse Ref-8 v2.0 Ambion) or RIN score values for RNA-seq. Microarray data generation and primary microarray data analysis was described previously [12]. Microarray data was used for differential pathway analysis with Ingenuity IPA software (Ingenuity) and results were considered significant for *p*-values less than 0.05. Heat maps were then generated with MeV software using fold changes Log2(cKO/Ctrl). For RNA-Seq analysis, RNA integrity was analyzed with a 2100 Bioanalyzer with an RNA 6000 kit (Agilent Technologies). RNA-Seq libraries were prepared using the Illumina TruSeq v2 library preparation kit and sequenced with paired-end 50 bp reads on an Illumina HiSeq 4000 in biological duplicates.

For quantitative real-time polymerase chain reaction (rt-qPCR), cDNA was synthesized from ~0.5 μg RNA using the SuperScript III first strand synthesis system (Invitrogen) as described by the supplier and subjected to rt-qPCR amplification using the QuantiTect

SYBR-Green PCR Kit (Qiagen) and a 7300 or 7500 Real Time PCR system (Applied Biosystems) using the following conditions: 10 min 95°C followed by 45 cycles of 30 sec at 95°C, 30 sec at 60°C and 30 sec at 72°C. Relative mRNA levels were compared to the housekeeping gene *Gapdh* and determined with the ΔΔCt method. Primers for the analyzed genes are provided upon requests. All rt-qPCR assays were performed in triplicates.

Supplemental Figures

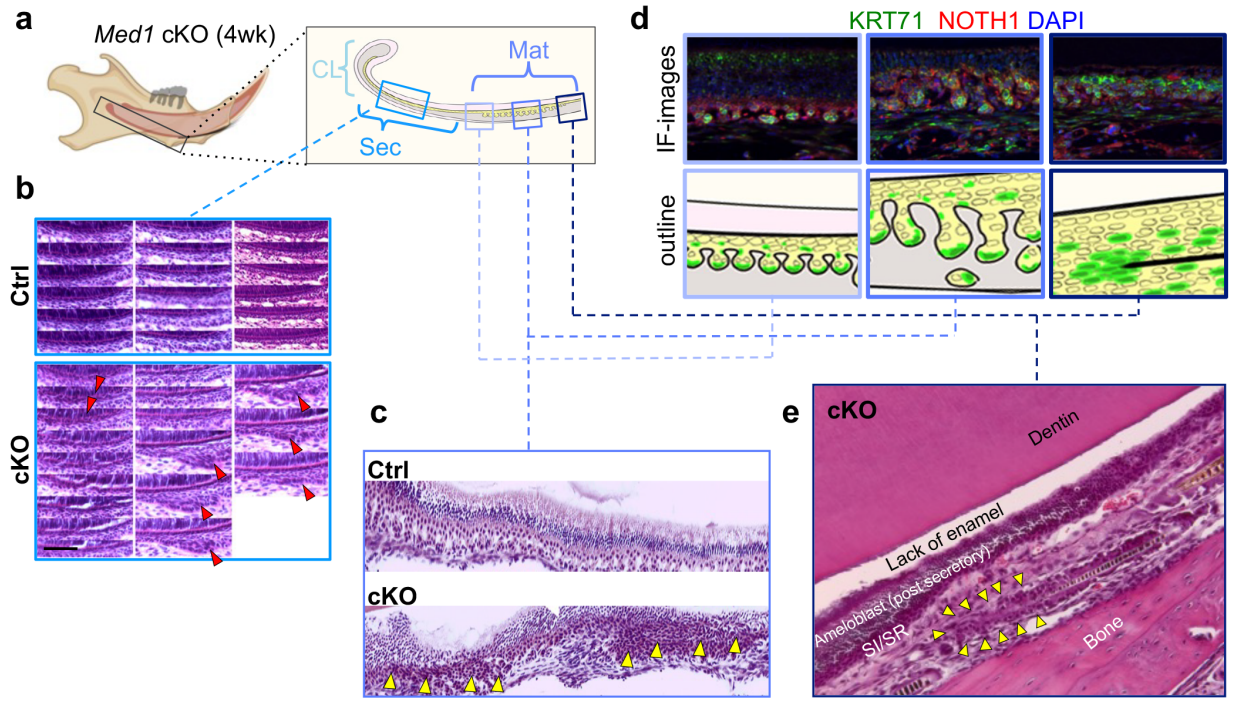

Suppl. Fig. 1: Histological and immuno-histological characterization of *Med1* cKO incisor tissue. a Diagram depicting the differentiation stages of mouse incisors including the location of the cervical loop (CL), the secretory stage (Sec) and the maturation stage (Mat) of dental epithelia. Right, detailed representation of Sec and Mat. **b** Serial sectioning showing progression of abnormal stratum intermedium (SI) development with generation of atypical cell clusters (red triangles) in *Med1* cKO mice. **c** H&E staining to show abnormal expansion of papillary layer in cKO (yellow triangles). **d** Top, immuno-fluorescent visualization of KRT17 (green), NOTCH1 (red) and DAPI counterstaining (blue) in SI/stellate reticulum (SR) derived papillary layers at 3 different locations of the Mat stage in *Med1* cKO mice. Bottom, diagram to show the locations of hair marker expression (green). **e** H&E-stained sections emphasizing the location of hair generating cell cluster found between dentin and bone in *Med1* cKO. SI, stratum intermedium, SR stellate reticulum.

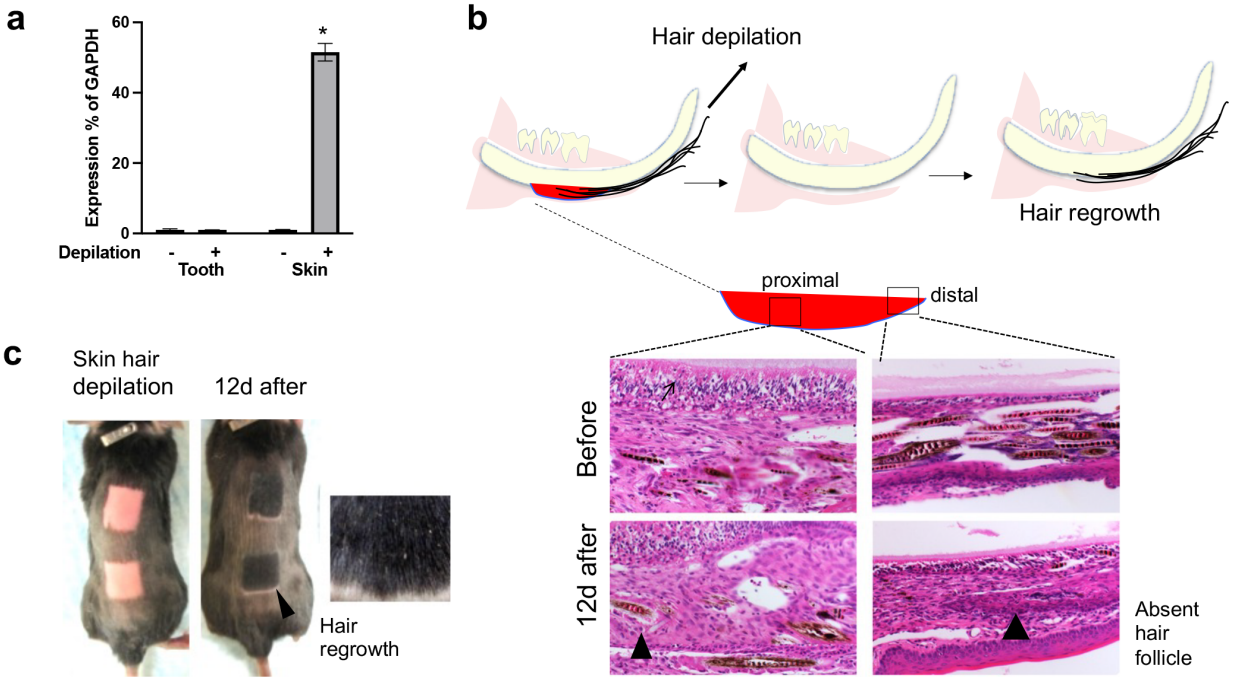

Suppl. Fig. 2: Effects of hair depilation on dental hair regeneration. a Hair marker *Krt31* mRNA expression in CL tissues of *Med1* cKO mice (tooth, left) and in normal skin tissue (skin right) before (-) and 8 days after (+) hair depilation. Representative data of average and SD of relative expression (% of GAPDH) and the statistical significance (n=3, * $p<0.05$). **b** Histological assessment of atypical hair generating cell clusters in *Med1* cKO incisors before and 12 days after hair depilation in proximal and distal region of the mandible (black triangles) corresponding to diagram. **c** Mouse skin shortly after hair depilation (left) and 12 days post depilation (right), when hair is regrown (arrow) and enlarged image of hair.

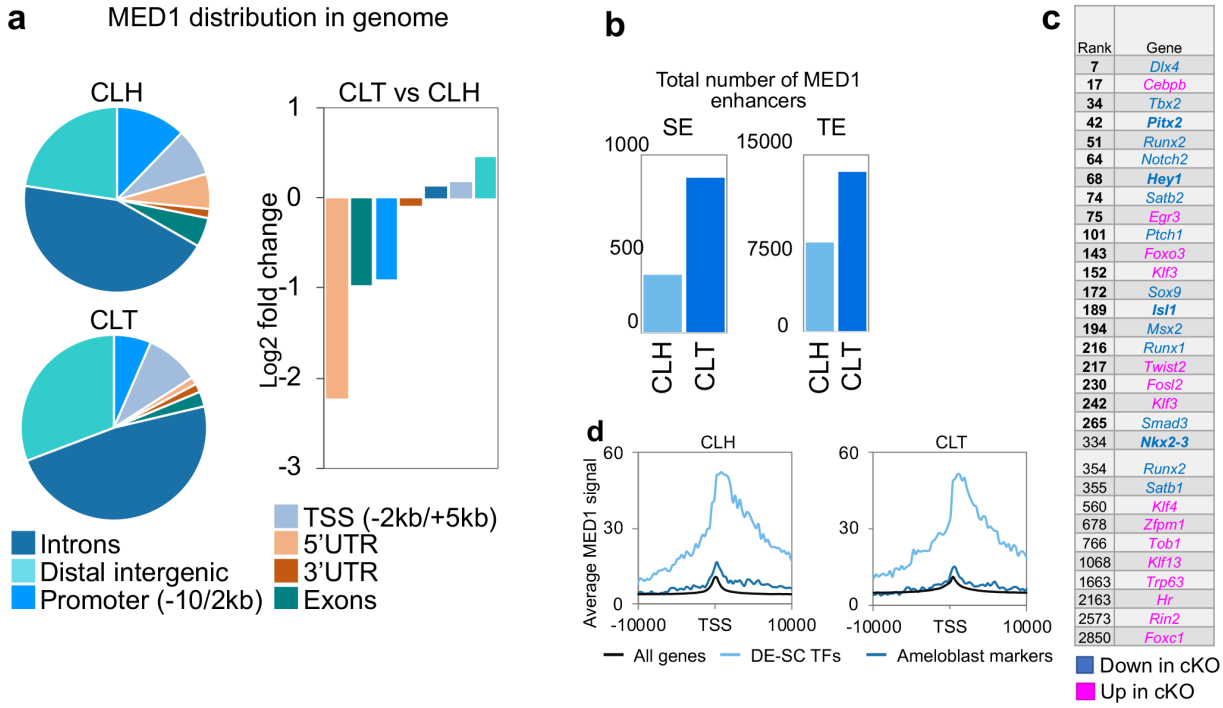

Suppl. Fig. 3: Med1 is distributed in different genomic regions in dental stem cells (CLH) and their progenies (CLT) in normal mice.

a Left, relative distribution of Med1 binding at different genomic elements in CLH and CLT Ctrl tissues (left); right, shift in Med1 binding at shown elements between CLT and CLH of Ctrl tissues (right) **b** Total number of super enhancers (SE) and typical enhancers (TE) in CLH and CLT Ctrl tissues. The 325 SEs and 871 SEs were identified in the CLH and CLT, respectively. **c** List of transcription factors regulated by Med1 containing enhancers in CLH. Enhancer ranking numbers is noted left and colors define regulation of mRNA expression in CLH upon loss of *Med1*. **d** Average Med1 occupancy at promoters (TSS +/- 10kbp) for enamel fate transcription factors (TFs) (pale blue line), ameloblast markers (blue line) and all other genes (black line) in CLH and CLT tissues.

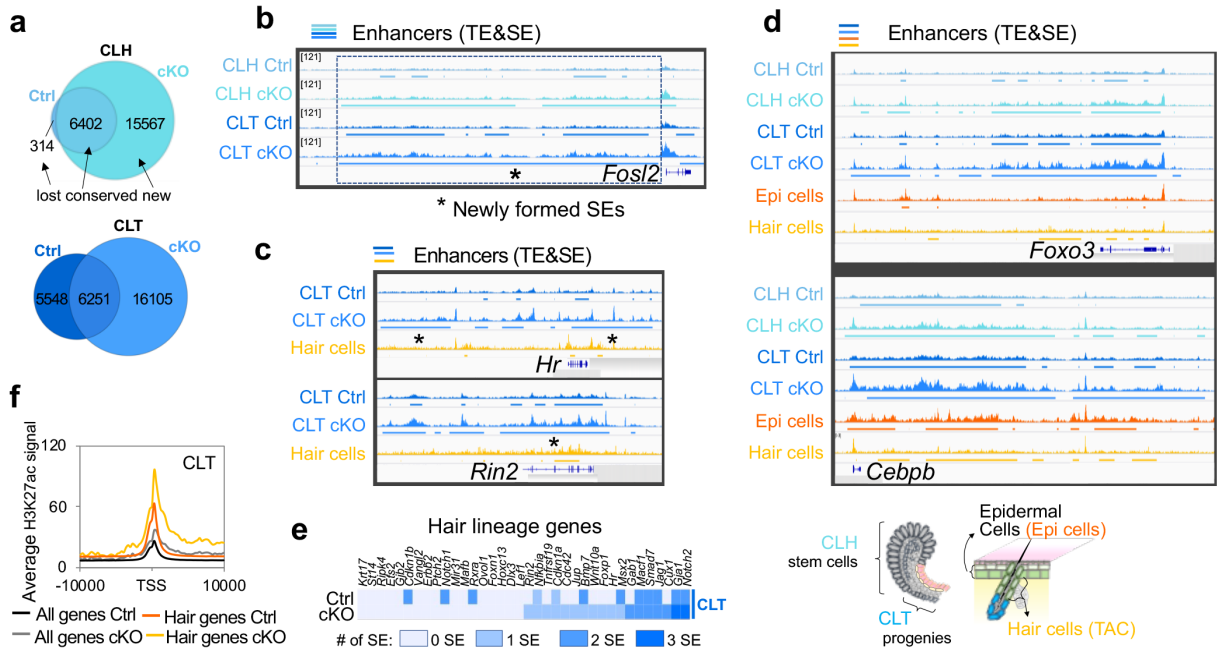

Suppl. Fig. 4: Genomic H3K27ac occupancy in promoters and enhancers and their changes in cKO dental tissues. a Numbers of typical enhancers (TEs) in Ctrl and cKO at CLH and CLT tissues. Lost, conserved and new TEs for cKO are shown. **b-d** H3K27ac occupancy around the loci of epidermal *Fosl2* (**b**), hair lineage driving *Hr* and *Rin2* (**c**), and epidermal transcription factors *Foxo3* and *Cebpb* (**d**) in Ctrl and *Med1* cKO at CLH and CLT tissues. Newly formed super-enhancers (SEs) in cKO are marked with asterisks (*). These enhancer profiles are compared with enhancer profiles (H3K27ac) from skin derived epidermal cells (Epi cells) and hair follicle transient amplifying (TAC) cells (Hair cells), in which locations of dental and skin epithelia are inserted. **e** Number of H3K27ac super-enhancers around genomic loci for hair lineage genes after *Med1* loss in CLT tissues. **f** Average H3K27ac occupancy at promoters (TSS +/- 10kbp) for hair lineage genes in CLT tissues in *Med1* cKO and Ctrl mice**.**

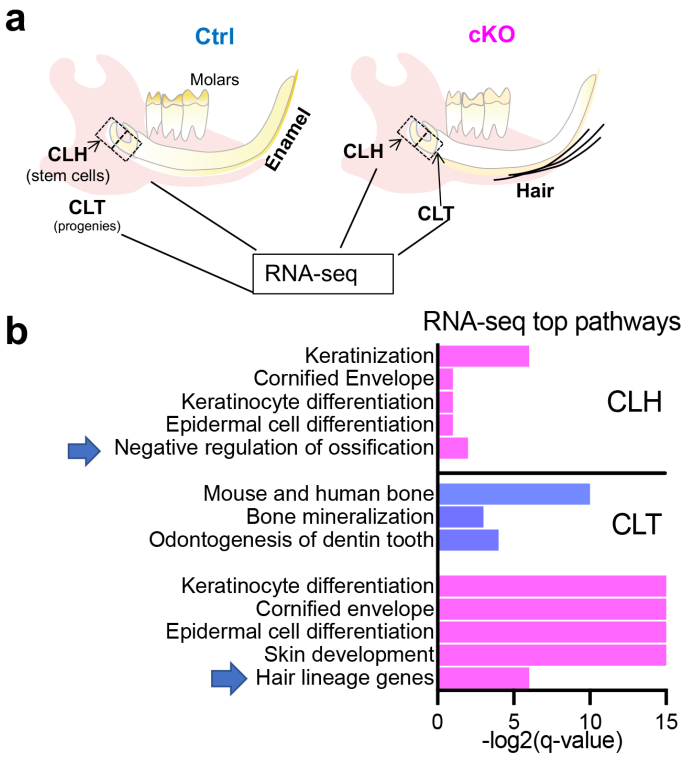

Suppl. Fig. 5: Functional annotation for differentially expressed genes in *Med1* cKO versus Ctrl dental stem cells (CLH) and their progenies (CLT). **a** Top, schematic diagram illustrating the collected tissues for the RNA-Seq experiment using two litters of 4 weeks-old Med1 cKO and Ctrl mice. **b** GO-based annotations representing up-regulated gene sets are shown in pink, down-regulated gene sets are shown in blue. Blue arrows show relevant pathways for hair formation (bottom) and enamel dysplasia (top) observed in *Med1* cKO mice.

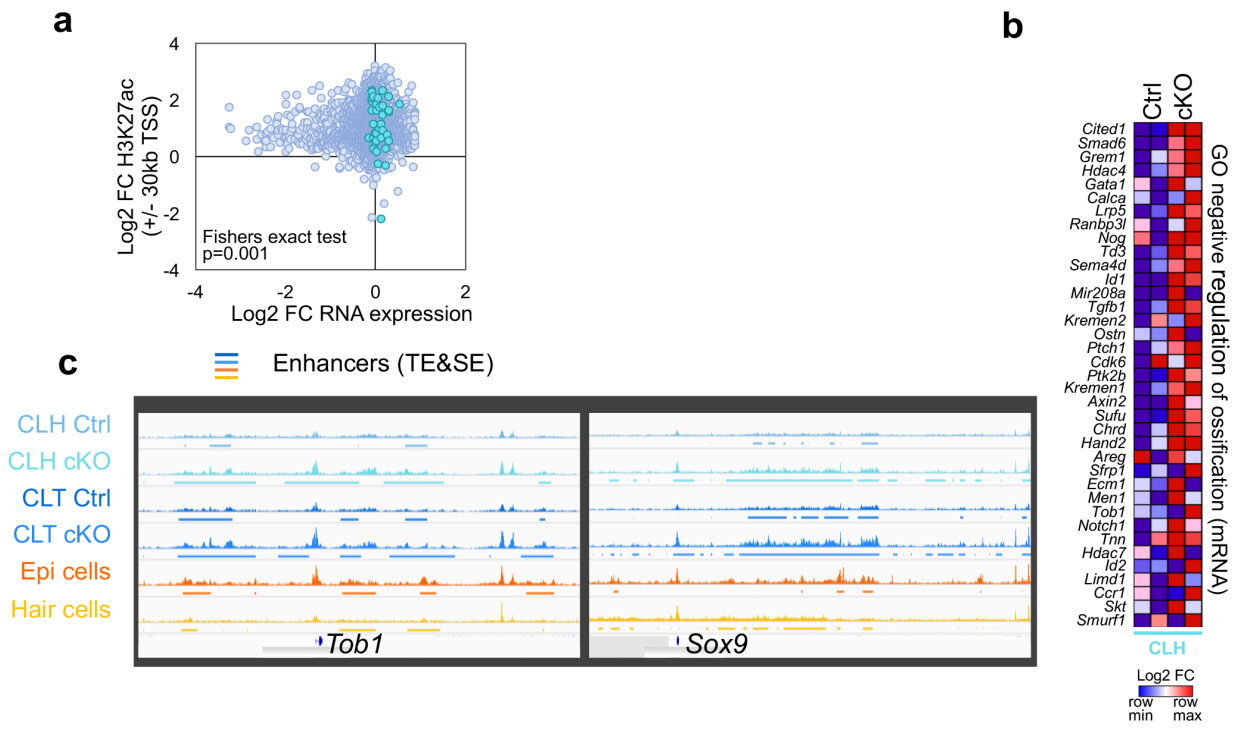

Suppl. Fig. 6: Loss of Med1 perturbs ossification pathways in dental tissues. a Correlation between gene expression and H3K27ac promoter occupancy (TSS +/-30 kb) in *Med1* cKO vs Ctrl CLT tissues. Blue dots highlight the gene-set 'negative regulation of ossification', pale blue dots represent all other genes. **b** Heatmap showing the changes is RNA expression for the gene set 'Go negative regulation of ossification' in Ctrl and *Med1* cKO CLH tissues. **c** Chip-seq enhancer profiles (H3K27ac) around loci of ossification inhibitors *Tob1 and Sox9.* Here, enhancers (colored underlines) expand in size or heights after loss of *Med1* cKO in CLH and CLT tissues. As a comparison, H3K27ac profiles for skin derived epidermal cells (Epi cells) and hair follicle TAC cells (Hair cells) are shown.